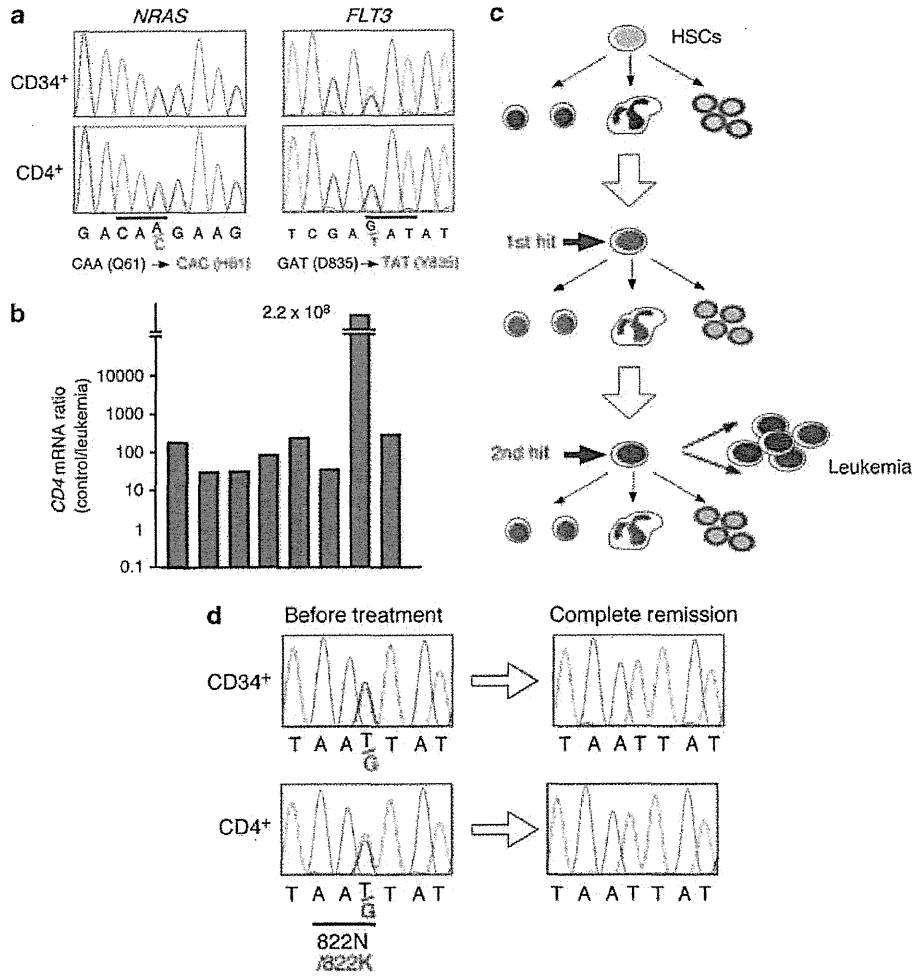

Figure 4 Proposed stepwise nature of leukemogenesis. (**a**) Sequencing electrophoretograms for the regions surrounding codon 61 of *NRAS* or codon 835 of *FLT3* in genomic DNA from the CD34$^+$ and CD4$^+$ fractions of patient IDs JM17 and JM08, respectively. Heterozygous nucleotide changes that give rise to NRAS(Q61H) or FLT3(D835Y) were detected in both fractions of the corresponding patients. (**b**) The amount of *CD4* mRNA in the CD4$^+$ (control) and CD34$^+$ (leukemia) fractions of leukemia patients (with a substantial amount of control *GAPDH* mRNA) was quantitated by reverse transcription and real-time PCR analysis and expressed as the control/leukemia ratio. (**c**) Hematopoietic stem cells (HSCs) give rise to a wide range of mature blood cells. Even after the first hit (mutation) of the genome, HSCs retain their full differentiation capacity, and therefore produce differentiated cells harboring this first hit. After the second hit, the affected cell fraction undergoes full transformation to leukemia. (**d**) Sequencing electrophoretograms for the genome of CD34$^+$ and CD4$^+$ fractions from patient ID JM03 showing a heterozygous mutation for KIT(N822K) before chemotherapy but not after.

between steps (Figure 4c). If a first hit occurs in the genome of hematopoietic stem (or progenitor) cells and if such a somatic change does not result directly in the generation of full-blown leukemia, the preleukemic clones may give rise to terminally differentiated blood cells (including CD4$^+$ cells). After a certain period, a second (or possibly a third) hit occurs in the immature cells and triggers the rapid growth of leukemic clones without differentiation. In such a scenario, terminally differentiated 'normal' cells may still harbor the first hit in their genome.

Support for this latter possibility was provided by patient ID JM03, who had AML (M2 subtype) with a t(8;21) chromosome anomaly. Before chemotherapy, the genomic DNA of both CD34$^+$ and CD4$^+$ fractions from this patient harbored a heterozygous mutation of *KIT* that results in the production of a constitutively activated mutant protein, KIT(N822K) (Shimada *et al.*, 2006) (Figure 4d). The same change was also detected in cDNA prepared from the CD34$^+$ fraction (data not shown). Leukemic blasts in this patient were sensitive to standard chemotherapeutic regimens, and the patient underwent complete remission. Examination of CD34$^+$ and CD4$^+$ fractions obtained during the remission period revealed that the N822K codon change was no longer detectable not only in the CD34$^+$ fraction but also in the CD4$^+$ fraction (Figure 4d). These data thus support the scenario shown in Figure 4c: The N822K

change represents the first hit and was present in differentiated blood cells, and the corresponding pre-leukemic clones were simultaneously eradicated together with the leukemic clones by chemotherapy.

On the other hand, as shown in Supplementary Tables S1 and S2, a heterozygous mutation for NRAS(G12S) was found only in the $CD34^+$ fraction, but not in the $CD4^+$ fraction of the patient ID JM16. Conventional chemotherapy for this patient eradicated the leukemic blasts carrying the mutation (Supplementary Figure S7), also confirming that a successful treatment results in the disappearance of cells with a (possible) 'second hit'.

Our hypothesis of the stepwise leukemogenesis is also consistent with the previous detection of the *RUNX1-CBFA2T1* oncogene in differentiated blood cells (Kwong *et al.*, 1996; Miyamoto *et al.*, 1996, 2000).

Discussion

Our large-scale genomic resequencing of human leukemia specimens with DNA microarrays has identified recurrent nucleotide changes responsible for the generation of JAK3 and DNMT3A mutants. Whereas JAK3 mutants were unexpectedly found in adult AML, their transforming ability, and possibly their contribution to leukemogenesis, varied substantially. However, our bone marrow transplantation experiments showed that at least one of these JAK3 mutants (M511I) directly participates in the development of leukemia. Identification of the M511I mutation of JAK3 in the leukemic fraction but not in the control fraction of patient ID JM07 suggests that this mutation may be the second hit triggering AML. Given that the blasts of this patient had a normal karyotype, it is likely that the first hit is present in the genome of both fractions. Karyotyping of other patients with *JAK3* mutations showed a total of three cases with a normal karyotype, one case with t(8;21), and one case with a numerical anomaly of several chromosomes (Supplementary Table S3), suggesting that *JAK3* mutations may be preferentially associated with leukemia with a normal karyotype.

Although JAK3(M511I) was identified in AML, our bone marrow transplantation experiments with hematopoietic stem cells expressing this mutant yielded T-cell acute lymphoblastic leukemia. In contrast to human leukemia, in which JAK3 changes may constitute a second hit (probably in progenitor cells), JAK3(M511I) may have been expressed in all hematopoietic cells of the recipient mice. JAK3(M511I) thus likely triggered leukemia within a T-cell fraction the intracellular context of which is optimized for JAK3 signaling.

It has been frequently observed that transgenic mouse or bone marrow transplantation experiments for leukemic oncogenes do not accurately recapitulate the original leukemia subtypes (Wong and Witte, 2001). Transgenic mice expressing $p210^{BCR\text{-}ABL1}$, for instance, usually develop T-cell lymphoma or acute lymphoblastic leukemia, not chronic myeloid leukemia. Furthermore, bone marrow transplantation with hematopoietic progenitor cells expressing $p210^{BCR\text{-}ABL1}$ often leads to development of lymphoma, AML, acute lymphoblastic leukemia or macrophage tumors. Generation of malignancy in such systems may, thus, be elaborately influenced by mouse strains, promoter fragments for artificial expression and/or cell types to be used for gene transduction.

Our detection of recurrent DNMT3A hypomorphic mutations in leukemia clones may indicate the presence of an abnormal methylation profile in the genome of such blasts. However, given the limited amount of the specimens available, we were able to investigate microsatellite stability only at certain loci (Koinuma *et al.*, 2005), revealing no apparent microsatellite instability (data not shown). We also generated BA/F3 cells expressing wild-type or R882H forms of DNMT3A to compare the methylation status of some CpG islands in the genome; again, we detected no discernable differences between the two cell preparations (data not shown). However, given that BA/F3 cells contained two copies of wild-type *Dnmt3a* in addition to multiple copies of mutant *DNMT3A*, whereas the leukemic blasts likely harbor one copy each of the wild-type and mutant *DNMT3A* alleles, the clinical relevance of the R882 mutant requires further examination under the latter condition. Cell proliferation/differentiation is indeed influenced substantially by the copy number of *DNMT3* genes (Okano *et al.*, 1999; Ehrlich, 2003).

Our observations indicate the importance of preparing paired normal fractions in large-scale resequencing projects, but they also reveal a difficulty in the preparation of *bona fide* 'normal' fractions in the case of leukemic disorders. Our data thus indicate that nonleukemic blood cells may harbor early genomic hits, rendering them inappropriate as controls. Furthermore, a substantial proportion of fingernail DNA was recently shown to be derived from donor cells among recipients of allogeneic stem cell transplants (Imanishi *et al.*, 2007), indicating that nonblood cells may contain DNA derived from transplanted cells. Therefore, it is possible that buccal, fingernail or even hair cells may not be suitable as normal cell controls. In contrast to solid tumors, for which blood cells are appropriate as paired normal fractions, leukemic disorders require that caution be taken to discriminate somatic nucleotide changes from germline polymorphisms.

Materials and methods

Wafer sequencing

$CD34^+$ and $CD4^+$ fractions were isolated from leukemic individuals using CD34microbeads and CD4microbeads, respectively, and a MidiMACS separator (Miltenyi Biotec, Gladbach, Germany). All clinical specimens were obtained with written informed consent, and the study was approved by the ethics committees of both the Jichi Medical University and the Nagasaki University. DNA sequencing wafers were designed and processed at Perlegen Sciences. Genes to be interrogated on the wafers were selected from the Entrez Gene database (http://www.ncbi.nlm.nih.gov/sites/entrez?db=gene)

by searching with various keywords characteristic to each subcategory (such as DNA repair, regulation of chromatin structure, etc.), followed by manual inspection. The final gene list for the wafers is shown in Supplementary Table S6. Construction of the wafers, quality control analysis and data processing are described in Supplementary Text.

JAK3 analysis

Complementary DNAs for JAK3 mutants were generated using a QuikChange site-directed mutagenesis kit (Stratagene, La Jolla, CA, USA) and ligated into the pMX retroviral vector (Onishi *et al.*, 1996). Ecotropic recombinant retroviruses encoding each mutant were produced in BOSC23 cells transfected with the corresponding pMX-based plasmid and were used to infect BA/F3 or 32D cells as described previously (Choi *et al.*, 2007). Both types of cell were cultured in RPMI 1640 medium supplemented with 10% fetal bovine serum (both from Life Technologies, Carlsbad, CA, USA) and mouse IL-3 (Sigma, St Loius, MO, USA) at 10 Units/ml; differentiation of 32D cells was induced by culture in the presence of serum and mouse granulocyte colony-stimulating factor (Sigma) at 0.5 ng/ml. A concentrated preparation of a retrovirus with a VSV-G envelope and encoding both JAK3(M511I) and enhanced green fluorescent protein was used to infect $CD34^-$ c-Kit^+ Sca-1^+ Lineage-$marker^-$ ($CD34^-$KSL) hematopoietic stem cells isolated from the bone marrow of C57BL/6 mice, and the infected cells were transplanted into lethally irradiated mice congenic for the *Ly5* locus (Iwama *et al.*, 2004). *CD4*, *JAK2* and *JAK3* mRNAs were quantitated by reverse transcription and real-time PCR analysis using an ABI7900HT system (Life Technologies) and with the primers 5′-CTGGAATCCAACATCAAGGTTCTG-3′ and 5′-AATTGTAGAGGAGGCGAACAGGAG-3′ for CD4, 5′-CTCCAGAATCACTGACAGAGAGCA-3′ and 5′-CCAC TCGAAGAGCTAGATCCCTAA-3′ for *JAK2* and 5′-GAGC TCTTCACCTACTGCGACAAA-3′ and 5′-AGCTATGAAA AGGACAGGGAGTGG-3′ for JAK3; the cDNA for GAPDH (glyceraldehyde-3-phosphate dehydrogenase) was also amplified with the primers 5′-GTCAGTGGTGGACC TGACCT-3′ and 5′-TGAGCTTGACAAAGTGGTCG-3′. The relative abundance of the cDNAs of interest was calculated from the threshold cycle (C_T) for each cDNA and that for *GAPDH* cDNA.

DNMT3A analysis

Recombinant His_6-tagged DNMT3A or DNMT3A(R882H) was expressed in SF9 cells using the Bac-to-Bac baculovirus expression system (Invitrogen, Carlsbad, CA, USA), and each protein was purified by stepwise column chromatography as described previously (Suetake *et al.*, 2003). The enzymatic activity of each protein was assayed with -*S*-adenosyl-L-methionine (GE Healthcare, Waukesha, WI, USA) and dIdC or dGdC as substrates (Suetake *et al.*, 2003). The association between Myc epitope-tagged human DNMT3L and wild-type or R882H forms of human DNMT3A in transfected HEK293 cells was examined by immunoprecipitation and immunoblot analyses.

Conflict of interest

The authors declare no conflict of interest.

Acknowledgements

We thank D Cox, KA Frazer, DG Ballinger, J Montgomery, H Tao, C Chen, L Stuve, J Kwon, J Sheehan and Y Zhan for discussion on the wafer experiments, as well as JN Ihle, T Kitamura and SB Baylin for human *JAK3* cDNA, the pMX plasmid and human *DNMT3A* cDNA, respectively. This study was supported in part by a grant for Third-Term Comprehensive Control Research for Cancer from the Ministry of Health, Labor, and Welfare of Japan, and by a grant for Scientific Research on Priority Areas 'Applied Genomics' from the Ministry of Education, Culture, Sports, Science, and Technology of Japan.

References

Bentley DR, Balasubramanian S, Swerdlow HP, Smith GP, Milton J, Brown CG *et al.* (2008). Accurate whole human genome sequencing using reversible terminator chemistry. *Nature* **456**: 53–59.

Byrd JC, Mrozek K, Dodge RK, Carroll AJ, Edwards CG, Arthur DC *et al.* (2002). Pretreatment cytogenetic abnormalities are predictive of induction success, cumulative incidence of relapse, and overall survival in adult patients with *de novo* acute myeloid leukemia: results from cancer and leukemia Group B (CALGB 8461). *Blood* **100**: 4325–4336.

Choi YL, Kaneda R, Wada T, Fujiwara S, Soda M, Watanabe H *et al.* (2007). Identification of a constitutively active mutant of JAK3 by retroviral expression screening. *Leuk Res* **31**: 203–209.

Ehrlich M. (2003). The ICF syndrome, a DNA methyltransferase 3B deficiency and immunodeficiency disease. *Clin Immunol* **109**: 17–28.

El-Osta A. (2004). The rise and fall of genomic methylation in cancer. *Leukemia* **18**: 233–237.

Greenberger JS, Sakakeeny MA, Humphries RK, Eaves CJ, Eckner RJ. (1983). Demonstration of permanent factor-dependent multipotential (erythroid/neutrophil/basophil) hematopoietic progenitor cell lines. *Proc Natl Acad Sci USA* **80**: 2931–2935.

Greenman C, Stephens P, Smith R, Dalgliesh GL, Hunter C, Bignell G *et al.* (2007). Patterns of somatic mutation in human cancer genomes. *Nature* **446**: 153–158.

Grimwade D, Walker H, Oliver F, Wheatley K, Harrison C, Harrison G *et al.* (1998). The importance of diagnostic cytogenetics on outcome in AML: analysis of 1612 patients entered into the MRC AML 10 trial. The Medical Research Council Adult and Children's Leukaemia Working Parties. *Blood* **92**: 2322–2333.

Imanishi D, Miyazaki Y, Yamasaki R, Sawayama Y, Taguchi J, Tsushima H *et al.* (2007). Donor-derived DNA in fingernails among recipients of allogeneic hematopoietic stem-cell transplants. *Blood* **110**: 2231–2234.

Iwama A, Oguro H, Negishi M, Kato Y, Morita Y, Tsukui H *et al.* (2004). Enhanced self-renewal of hematopoietic stem cells mediated by the polycomb gene product Bmi-1. *Immunity* **21**: 843–851.

Jia D, Jurkowska RZ, Zhang X, Jeltsch A, Cheng X. (2007). Structure of Dnmt3a bound to Dnmt3L suggests a model for *de novo* DNA methylation. *Nature* **449**: 248–251.

Kiyoi H, Yamaji S, Kojima S, Naoe T. (2007). JAK3 mutations occur in acute megakaryoblastic leukemia both in Down syndrome children and non-Down syndrome adults. *Leukemia* **21**: 574–576.

Koinuma K, Kaneda R, Toyota M, Yamashita Y, Takada S, Choi YL *et al.* (2005). Screening for genomic fragments that are methylated specifically in colorectal carcinoma with a methylated MLH1 promoter. *Carcinogenesis* **26**: 2078–2085.

Kralovics R, Passamonti F, Buser AS, Teo SS, Tiedt R, Passweg JR *et al.* (2005). A gain-of-function mutation of JAK2 in myeloproliferative disorders. *N Engl J Med* **352**: 1779–1790.

Kubonishi I, Miyoshi I. (1983). Establishment of a Ph1 chromosome-positive cell line from chronic myelogenous leukemia in blast crisis. *Int J Cell Cloning* **1**: 105–117.

Kwong YL, Wong KF, Chan V, Chan CH. (1996). Persistence of AML1 rearrangement in peripheral blood cells in t(8;21). *Cancer Genet Cytogenet* **88**: 151–154.

Ley TJ, Mardis ER, Ding L, Fulton B, McLellan MD, Chen K *et al.* (2008). DNA sequencing of a cytogenetically normal acute myeloid leukaemia genome. *Nature* **456**: 66–72.

Miyamoto T, Nagafuji K, Akashi K, Harada M, Kyo T, Akashi T *et al.* (1996). Persistence of multipotent progenitors expressing AML1/ETO transcripts in long-term remission patients with t(8;21) acute myelogenous leukemia. *Blood* **87**: 4789–4796.

Miyamoto T, Weissman IL, Akashi K. (2000). AML1/ETO-expressing nonleukemic stem cells in acute myelogenous leukemia with 8;21 chromosomal translocation. *Proc Natl Acad Sci USA* **97**: 7521–7526.

Nimer SD, Moore MA. (2004). Effects of the leukemia-associated AML1-ETO protein on hematopoietic stem and progenitor cells. *Oncogene* **23**: 4249–4254.

Okano M, Bell DW, Haber DA, Li E. (1999). DNA methyltransferases Dnmt3a and Dnmt3b are essential for *de novo* methylation and mammalian development. *Cell* **99**: 247–257.

Onishi M, Kinoshita S, Morikawa Y, Shibuya A, Phillips J, Lanier LL *et al.* (1996). Applications of retrovirus-mediated expression cloning. *Exp Hematol* **24**: 324–329.

Patil N, Berno AJ, Hinds DA, Barrett WA, Doshi JM, Hacker CR *et al.* (2001). Blocks of limited haplotype diversity revealed by high-resolution scanning of human chromosome 21. *Science* **294**: 1719–1723.

Pikman Y, Lee BH, Mercher T, McDowell E, Ebert BL, Gozo M *et al.* (2006). MPLW515L is a novel somatic activating mutation in myelofibrosis with myeloid metaplasia. *PLoS Med* **3**: e270.

Russell SM, Tayebi N, Nakajima H, Riedy MC, Roberts JL, Aman MJ *et al.* (1995). Mutation of Jak3 in a patient with SCID: essential role of Jak3 in lymphoid development. *Science* **270**: 797–800.

Sato T, Toki T, Kanezaki R, Xu G, Terui K, Kanegane H *et al.* (2008). Functional analysis of JAK3 mutations in transient myeloproliferative disorder and acute megakaryoblastic leukaemia accompanying Down syndrome. *Br J Haematol* **141**: 681–688.

Schlenk RF, Dohner K, Krauter J, Frohling S, Corbacioglu A, Bullinger L *et al.* (2008). Mutations and treatment outcome in cytogenetically normal acute myeloid leukemia. *N Engl J Med* **358**: 1909–1918.

Schwonzen M, Diehl V, Dellanna M, Staib P. (2007). Immunophenotyping of surface antigens in acute myeloid leukemia by flow cytometry after red blood cell lysis. *Leuk Res* **31**: 113–116.

Shimada A, Taki T, Tabuchi K, Tawa A, Horibe K, Tsuchida M *et al.* (2006). KIT mutations, and not FLT3 internal tandem duplication, are strongly associated with a poor prognosis in pediatric acute myeloid leukemia with t(8;21): a study of the Japanese Childhood AML Cooperative Study Group. *Blood* **107**: 1806–1809.

Sjoblom T, Jones S, Wood LD, Parsons DW, Lin J, Barber TD *et al.* (2006). The consensus coding sequences of human breast and colorectal cancers. *Science* **314**: 268–274.

Suetake I, Miyazaki J, Murakami C, Takeshima H, Tajima S. (2003). Distinct enzymatic properties of recombinant mouse DNA methyltransferases Dnmt3a and Dnmt3b. *J Biochem* **133**: 737–744.

Tallman MS, Altman JK. (2008). Curative strategies in acute promyelocytic leukemia. *Hematol Am Soc Hematol Educ Program* **2008**: 391–399.

Walters DK, Mercher T, Gu TL, O'Hare T, Tyner JW, Loriaux M *et al.* (2006). Activating alleles of JAK3 in acute megakaryoblastic leukemia. *Cancer Cell* **10**: 65–75.

Wheeler DA, Srinivasan M, Egholm M, Shen Y, Chen L, McGuire A *et al.* (2008). The complete genome of an individual by massively parallel DNA sequencing. *Nature* **452**: 872–876.

Wong S, Witte ON. (2001). Modeling Philadelphia chromosome positive leukemias. *Oncogene* **20**: 5644–5659.

Yamamoto Y, Kiyoi H, Nakano Y, Suzuki R, Kodera Y, Miyawaki S *et al.* (2001). Activating mutation of D835 within the activation loop of FLT3 in human hematologic malignancies. *Blood* **97**: 2434–2439.

Supplementary Information accompanies the paper on the Oncogene website (http://www.nature.com/onc)

Am J Physiol Heart Circ Physiol 299: H713–H722, 2010.
First published June 11, 2010; doi:10.1152/ajpheart.00273.2010.

Stress signaling by Tec tyrosine kinase in the ischemic myocardium

Michael J. Zhang,[1] Sarah Franklin,[1] Yifeng Li,[1] Sujing Wang,[1] Xiaochen Ru,[1] Scherise A. Mitchell-Jordan,[1] Hiroyuki Mano,[4] Enrico Stefani,[1,3] Peipei Ping,[2,3] and Thomas M. Vondriska[1,2,3]

Departments of [1]Anesthesiology, [2]Medicine, and [3]Physiology, David Geffen School of Medicine, University of California, Los Angeles, California; and [4]Division of Functional Genomics, Jichi Medical University, Tochigi, Japan

Submitted 18 March 2010; accepted in final form 2 June 2010

Zhang MJ, Franklin S, Li Y, Wang S, Ru X, Mitchell-Jordan SA, Mano H, Stefani E, Ping P, Vondriska TM. Stress signaling by Tec tyrosine kinase in the ischemic myocardium. *Am J Physiol Heart Circ Physiol* 299: H713–H722, 2010. First published June 11, 2010; doi:10.1152/ajpheart.00273.2010.—Nonreceptor tyrosine kinases have an increasingly appreciated role in cardiac injury and protection. To investigate novel tasks for members of the Tec family of nonreceptor tyrosine kinases in cardiac phenotype, we examined the behavior of the Tec isoform in myocardial ischemic injury. Ischemia-reperfusion, but not cardiac protective agents, induced altered intracellular localization of Tec, highlighting distinct actions of this protein compared with other isoforms, such as Bmx, in the same model. Tec is abundantly expressed in cardiac myocytes and assumes a diffuse intracellular localization under basal conditions but is recruited to striated structures upon various stimuli, including ATP. To characterize Tec signaling targets in vivo, we performed an exhaustive proteomic analysis of Tec-binding partners. These experiments expand the role of the Tec family in the heart, identifying the Tec isoform as an ischemic injury-induced isoform, and map the subproteome of its interactors in isolated cells.

ischemia; tyrosine kinase; proteomics

NONRECEPTOR TYROSINE KINASES are key regulatory molecules in the heart. Src, the prototypical nonreceptor tyrosine kinase, participates in numerous signaling events in the heart: it is a critical component of cardiac protection against ischemia (9, 27) as well as physiological responses to ANG II receptor stimulation in the cardiovascular system (7). Focal adhesion kinase (FAK) has an established role in cardiac hypertrophy (5), in response to angiogenic stimuli (22), or in the setting of ischemic injury (8). Likewise, the roles of protein tyrosine kinase PYK2 in hypertrophy (11) and JAK in ischemic injury and cardiac protection have been previously described (31).

In contrast, the actions of the Tec family of nonreceptor kinases in the heart are less well characterized. Tec family members are known to govern lymphocyte proliferation and the responses of these cells to various forms of receptor stimulation. The Tec isoform, in particular, couples T cell receptor (TCR) activation to Ca^{2+} release and the mobilization of stress kinases (19). Recent studies have implicated another isoform of the Tec family, Bmx, in angiogenesis and stress response. Specifically, genetic loss-of-function studies have shown that Bmx participates in wound healing (18), promotes angiogenesis and prevents cell death in ischemic skeletal muscle (10), and is a necessary component of compensatory cardiac hypertrophy at the cell and organ level after transverse aortic banding (14). While these observations support a stress-activated role for the Bmx isoform, a role unique to the Tec isoform in the heart has not been characterized.

In T cells, Tec is activated by TCR/CD3 or CD28 ligation and interacts with the CD28 receptor via its SH3 domain (24). While its expression in primary T cells is lower than that of IL-2-inducible T cell kinase (Itk), Tec protein levels are significantly elevated upon T cell activation, and this change is sufficient to induce phospholipase C-γ phosphorylation and nuclear factor of activated T cells (26). Some investigations from noncardiac systems have revealed physical interactions between Tec and other signaling molecules. Tec interacts with c-Kit under the influence of stem cell factor in MO7E cells (24) and other nonreceptor tyrosine kinases such as Lyn, which phosphorylates Tec in vitro (13). JAK1/2, which coprecipitates with and phosphorylates Tec in 293T cotransfected cells (21), has been shown to regulate Tec in heterologous and cell-free systems. The SHIP family of inositol phosphatases can inhibit Tec kinase activity and prevent Tec membrane localization in Jurkat cells (25). Yet, to our knowledge, no unbiased analysis of Tec signaling partners has been carried out in any system.

In support of a role outside of the immune system, an examination of Tec tissue distribution via the Human Protein Atlas (3) revealed a broad tissue distribution, including expression in heart muscle and cardiac myocytes, in contrast to other Tec family members, which exhibited more restricted tissue distribution. The ramifications of Tec signaling in the intact heart, however, are unknown. To investigate the role of Tec in cardiac signaling and to evaluate whether, like Bmx, it is a stress-activated kinase in this setting, we undertook an extensive characterization of its intracellular actions and signaling partners. Our data reveal the subproteome of Tec interactors and demonstrate the activation of Tec after cardiac stress, setting the groundwork for further investigations of the signaling actions of this family of kinases in the cardiovascular system.

METHODS

Cloning and transfection. Mouse TecIV cDNA (94% amino acid homology) (13) was subcloned into pcDNA3 with and without the COOH-terminal FLAG tag (DYKDDDDK). Nontagged Tec was used as a negative control for all subsequent steps. Transfections of human embryonic kidney (HEK)-293 cells were performed with Lipofectamine 2000 (Invitrogen) according to the manufacturer's protocol in 100-mm dishes. Cells were harvested 48 h after transfection and lysed with immunoprecipitation buffer containing (in mM) 150 NaCl, 20 Tris·HCl (pH 7.4), 1 EDTA, 1 EGTA, 2.5 sodium pyrophosphate, 1 β-glycerophosphate, 1 Na_3VO_4, 1 PMSF, and 1 NaF with protease inhibitor cocktail (Roche) and 1% Triton X-100 alone or with 0.6% CHAPS.

Address for reprint requests and other correspondence: T. M. Vondriska, Depts. of Anesthesiology, Medicine, and Physiology, David Geffen School of Medicine, Univ. of California-Los Angeles, BH 557 CHS, 650 Charles Young Dr., Los Angeles, CA 90095 (e-mail: tvondriska@mednet.ucla.edu).

Purification of Tec-associated proteins. Transfected cell lysates were sonicated three times for 10 s and centrifuged at 16,000 *g* for 10 min. The supernatant was precleared with protein A/G beads (Santa Cruz Biotechnology) and nonimmune mouse IgG (Santa Cruz Biotechnology) for 1 h at 4°C. Two different methods were used to purify Tec complexes, with both methods using nontagged Tec as the negative control. For immunoprecipitation, precleared lysates were incubated with protein A/G beads and anti-FLAG-M2 antibody (Sigma) overnight at 4°C. After three washes with immunoprecipitation buffer, beads were resuspended in Laemmli buffer and boiled. For FLAG affinity pulldown, precleared lysates were passed 20 times over a 200-μl column containing anti-FLAG-M2 affinity gel (Sigma). After a wash with 10 column volumes, Tec complexes were eluted with 1 ml of 100 μg/ml 3×FLAG peptide (Sigma). The eluate was concentrated to 30 μl with a 3-kDa MWCO Centricon column (Sigma). Samples were run on 7% Tris-glycine gels and stained with Coomassie blue R250.

In-gel trypsin digestion. Purifications of FLAG-tagged Tec and nontagged Tec were run in adjacent lanes, and, after Coomassie blue staining, each lane was sectioned into ~15 bands. Gel bands were washed with 50 mM NH_4HCO_3-50% acetonitrile twice and once with acetonitrile. Gel bands were dried in a speedvac and incubated sequentially with 10 mM Tris(2-carboxy-ethyl)phosphine hydrochloride-10 mM DTT at 56°C and 100 mM iodoacetamide at room temperature. Afterward, gel bands were incubated with 20 ng/μl trypsin for 18 h. Digestion was halted with 5% trifluoroacetic acid. Gel bands were vortexed and sonicated to extract digested peptides. The final solution was dried and resuspended in mass spectrometry (MS) *buffer A* (2% acetonitrile and 0.1% formic acid).

MS analysis and protein identification. Digested peptides were separated by reverse-phase nanoflow liquid chromatography (LC) on an Eksigent HPLC and introduced by electrospray into a Thermo Fisher LTQ-Orbitrap mass spectrometer operating in data-dependent mode. Spectra were then searched with the SEQUEST algorithm against the IPI Human version 3.51 database, and proteins with the following criteria underwent further analysis (as discussed in RESULTS): ΔCN > 0.1 and Xcorr versus charge state >2 (+1), >3(+2), >4(+3), and >5(+4). No proteins were accepted on the basis of less than two peptides, and all spectra used for identification were manually inspected.

Bioinformatic analysis of Tec-associated proteins. The molecular weight, isoelectric point, and grand average of hydropathy of Tec-interacting subsets were calculated based on the Swiss-Prot ProtParam tool and in-house software. Disorder prediction was performed using DISOPRED2 software (29). The reported values for each protein are the percentage of the molecule that is disordered.

Myocardial ischemia-reperfusion surgery and infarct size analysis. All experiments involving animals were conducted following protocols approved by the University of California-Los Angeles Institutional Animal Care and Use Committee. Adult (8–12 wk old) male Balb/c mice were used for all experiments. Anesthesia was induced by an intraperitoneal injection of pentobarbital (50 mg/kg body wt), and mice were intubated and mechanically ventilated with 95% O_2-5% CO_2 for the duration of the surgical procedure. The animal's temperature was continuously measured rectally and maintained at 36.5–37.5°C. After a left thoracotomy between ribs three and four, the pericardium was opened, and a silk 8-0 suture was passed under the left anterior descending coronary artery (LAD) 1–3 mm from the tip of the left atrium. Ischemia was induced by ligation of this suture over a 2-mm section of polyethylene-10 tubing, which was placed between the suture and the artery. After 30 min of coronary artery occlusion, the suture was removed to allow reperfusion, and the chest wall was closed. After 24 h of coronary artery reperfusion, the animal was anesthetized with a lethal dose of pentobarbital, and the heart was stopped by an injection of a bolus of saturated KCl solution. The infarcted region was determined by retrograde perfusion through the aorta of a 1% solution of 2,3,5-triphenyltetrazolium chloride in phosphate buffer (pH 7.4, 37°C), and the risk region was delineated by 1% solution of blue dye perfusion after reocclusion of the LAD. The heart was then frozen and sectioned, and individual sections were photographed. Infarct size was measured by manual tracing using the ImageJ program and expressed as a percentage of the area at risk. All surgeries and image analyses were conducted by different individuals in a blinded fashion.

Administration of diethylenetriamine/nitric oxide. Mice were given the known cardiac protective agent diethylenetriamine (DETA)/nitric oxide (NO) as four consecutive intravenous boluses (0.1 mg/kg each), each separated by 25 min, or PBS (vehicle) (23, 28). Ischemic injury was induced 24 h later, as described above (see Fig. 2*A*).

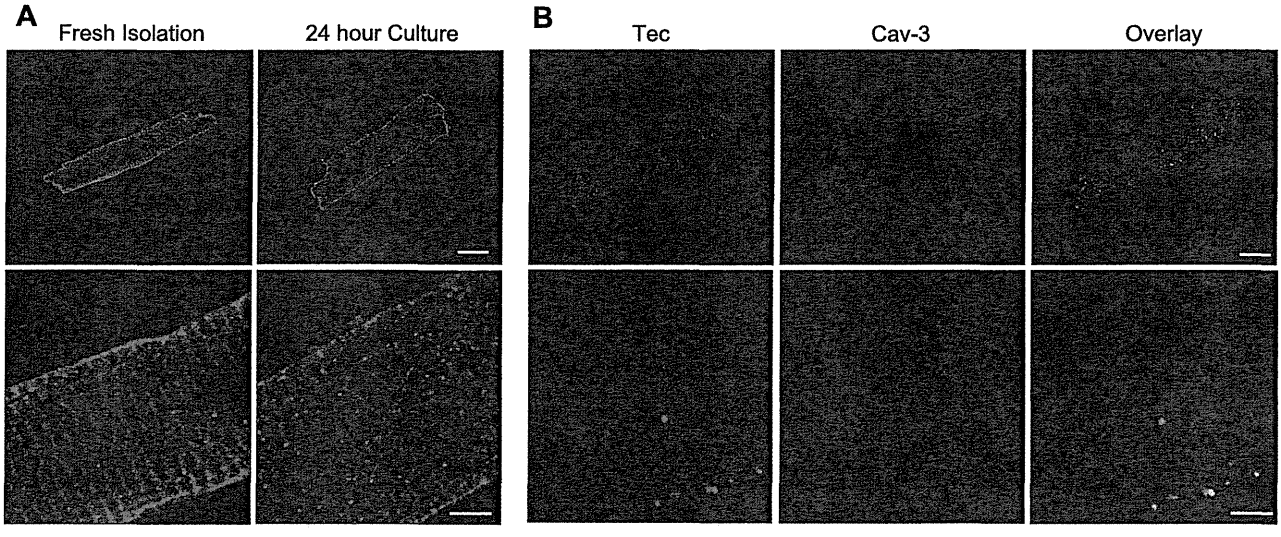

Fig. 1. Altered intracellular localization of Tec tyrosine kinase in adult cardiac myocytes. *A*: adult mouse myocytes were isolated by retrograde perfusion with collagenase and examined immediately (fresh isolation) or after 24 h in culture. Cells were fixed, and Tec was visualized by immunodecoration, demonstrating a striated localization pattern that returned to a dispersed, cytoplasmic arrangement after culture. *B*: colabeling with caveolin (Cav)-3 demonstrated the localization of Tec to T-tubules, a pattern that reverted to the diffuse cytoplasmic distribution after culture. Bar = 10 μM.

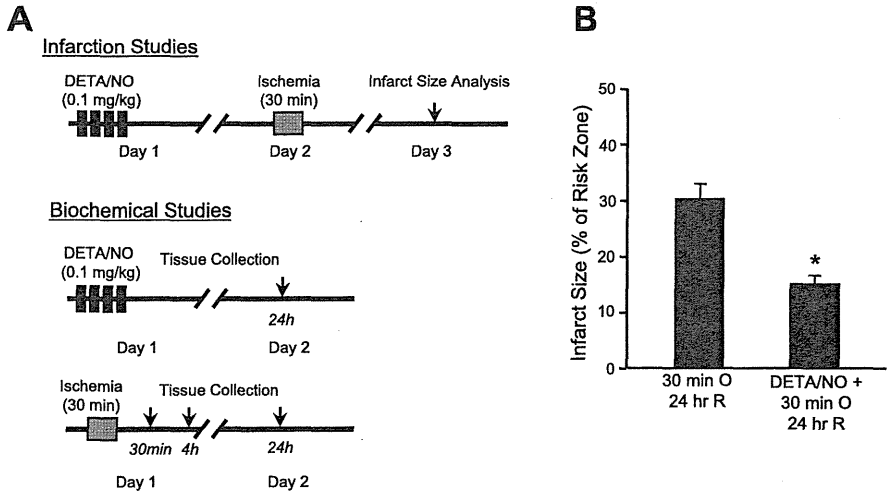

Fig. 2. Model of cardiac injury and protection. *A*: adult Balb/c mice were subjected to 30 min of left anterior descending coronary artery occlusion in the presence or absence of the cardioprotective reagent diethylenetriamine (DETA)/nitric oxide (NO). After 24 h of reperfusion, infarct size was measured by postmortem tetrazolium chloride staining in one cohort of mice, whereas hearts from the other cohort were excised for biochemical analysis. To investigate temporal changes in protein abundance after myocardial ischemia, tissue samples were also harvested after 30 min and 4 h of reperfusion in separate groups. *B*: infarct size analyses in control and preconditioned mice. Acute myocardial ischemia and reperfusion [occlusion (O) and reperfusion (R)] produced left ventricular infarction, which was significantly reduced by pretreatment with the NO donor DETA/NO. $n = 12$ mice/group. $^*P = 0.013$.

Myocyte isolation, culture, and stimulation. Adult cardiac myocytes were isolated using a protocol by O'Connell and colleagues (16) with minor modifications. Balb/c mice, injected 20 min before with 0.5 ml heparin, were killed, and their hearts were immediately excised and retrograde perfused with Tyrode solution followed by collagenase and type XI protease. The ventricular portion was taken and minced to separate cells. Additional filtering was done by gravity and a brief centrifugation, followed by calcium reintroduction and plating onto laminin-coated coverslips. For the overnight culture, cells were grown in DMEM (with Hanks balanced salts, 10% FBS, and 100 U/ml penicillin-streptomycin; 2% CO_2). Hypoxia was induced by placing the culture dishes in an air-tight chamber flushed for 5 min with 95% N_2-5% CO_2. Room air was reintroduced to induce reoxygenation. For purinergic stimulation, ATP was dissolved directly in PBS, and adenosine was first dissolved in DMSO and then in PBS.

Sucrose gradient ultracentrifugation of mouse hearts. Mouse hearts were homogenized with a dounce homogenizer in ice-cold immunoprecipation buffer containing 1% Triton X-100 (or with the addition of 0.6% CHAPS and 0.1% deoxycholate; 2 ml buffer/heart). Homogenates were mixed at 1:1.25 with 80% sucrose and laid at the bottom of ultracentrifuge tubes. Equal volumes of 35% sucrose and then 5% sucrose were overlaid. The resulting discontinuous gradient was centrifuged at 240,000 *g* for 18 h at 4°C, after which samples were immediately separated into eight fractions. Proteins were then

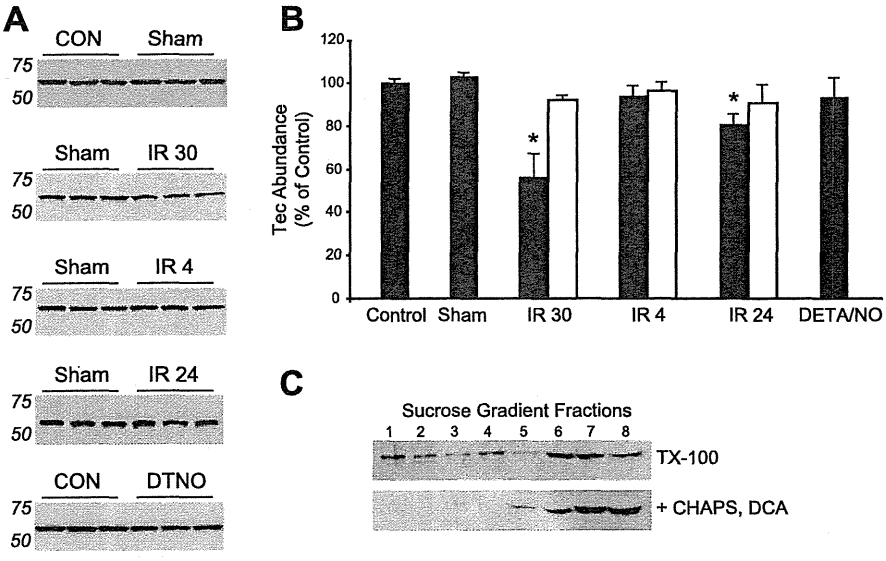

Fig. 3. Tec translocates to Triton X-100 (TX-100)-insoluble fractions after ischemia and reperfusion. *A*: Tec abundance was measured by Western blot analysis in ischemic and nonischemic regions of the same heart after solublization in Triton-X100 lysis buffer, which leaves lipid rafts insoluble. A significant decrease in Tec levels was detected after 30 min of ischemia and 30 min of reperfusion (IR 30 group) in the ischemic zone, whereas Tec was unchanged after 4 h of reperfusion (IR 4 group) and showed a smaller decrease after 24 h of reperfusion (IR 24 group). CON, control; Sham, mice subjected to sham operation; DTNO, DETA/NO treatment. $n = 3$ mice/group. *B*: quantified results from *A*. Importantly, these changes were only witnessed in the ischemic region of the heart (solid bars), not in the nonischemic region (open bars). No differences in basal Tec expression were detected between the base and apex of the heart (data not shown). DETA/NO treatment alone had no effect on Tec levels. $^*P < 0.05$ vs. control. *C*: use of zwitterionic (CHAPS) and ionic [deoxycholate (DCA)] detergents and ultracentrifugation demonstrated the raft association of Tec. *Fractions 1–8* were collected from the sucrose gradient representing the lowest to highest density. Note that in the absence of CHAPS and DCA, Tec was distributed across low-density fractions (*top* blot), indicative of insolubility, whereas additional detergents effectively extracted Tec from these low-density fractions (*bottom* blot).

chloroform-methanol precipitated and resuspended in Laemmli buffer for subsequent analyses.

Immunoblot analysis and densitometry. After SDS-PAGE separation, protein samples were transferred onto nitrocellulose membranes. Polyclonal anti-Tec (sc-1109) was purchased from Santa Cruz Biotechnology, and GAPDH was purchased from Abcam (loading control). Detection was performed with horseradish peroxidase-conjugated secondary antibodies along with the ECL detection system (GE Healthcare). Films underwent densitometric analysis with ImageJ.

Immunofluorescence-based confocal microscopy for in situ analysis of Tec localization. Isolated cardiomyocytes were plated on laminin-coated coverslips, cultured and stimulated as described above, fixed with paraformaldehyde, blocked in 5% milk and 1% serum, and incubated with anti-Tec or anti-caveolin-3 (Santa Cruz Biotechnology) overnight. Secondary antibody was added for 1 h, and, after a wash, coverslips were mounted on slides. Labeling was visualized with an Olympus Fluoview IX70 confocal microscope.

RESULTS

Tec exists in two distinct subcellular locations in cardiomyocytes. Previous investigations have demonstrated the expression of Tec in the rat heart, but the subcellular localization of this isoform in the mouse heart was unclear. We observed, by Western blot analysis, abundant expression of a single species of Tec protein in whole heart lysates as well as in isolated adult mouse cardiac myocytes. Tec expression was not significantly different in the atria or ventricles or in the base or apex of the heart (data not shown), as will become germane below in the analysis of the injured myocardium. To evaluate Tec subcellular localization in cardiac cells, we used antibody labeling and confocal microscopy. After calcium reintroduction, myocytes were either immediately fixed with paraformaldehyde or cultured for 24 h and then fixed. Interestingly, freshly isolated cardiac cells exhibited a striated Tec expression pattern (Fig. 1*A*; confirmed by caveolin-3 colocalization in Fig. 1*B*) that returned, after 24 h of culture, to a diffuse cytoplasmic localization (Fig. 1*A*). Based on these observations, we reasoned that the transient striated localization may be the result of the stress of isolation and that the cytoplasmic pattern is the endogenous basal state of Tec localization (in agreement with this conclusion, the analysis of Tec localization in cardiac tissue sections revealed a diffuse, nonstriated, cytoplasmic distribution; see

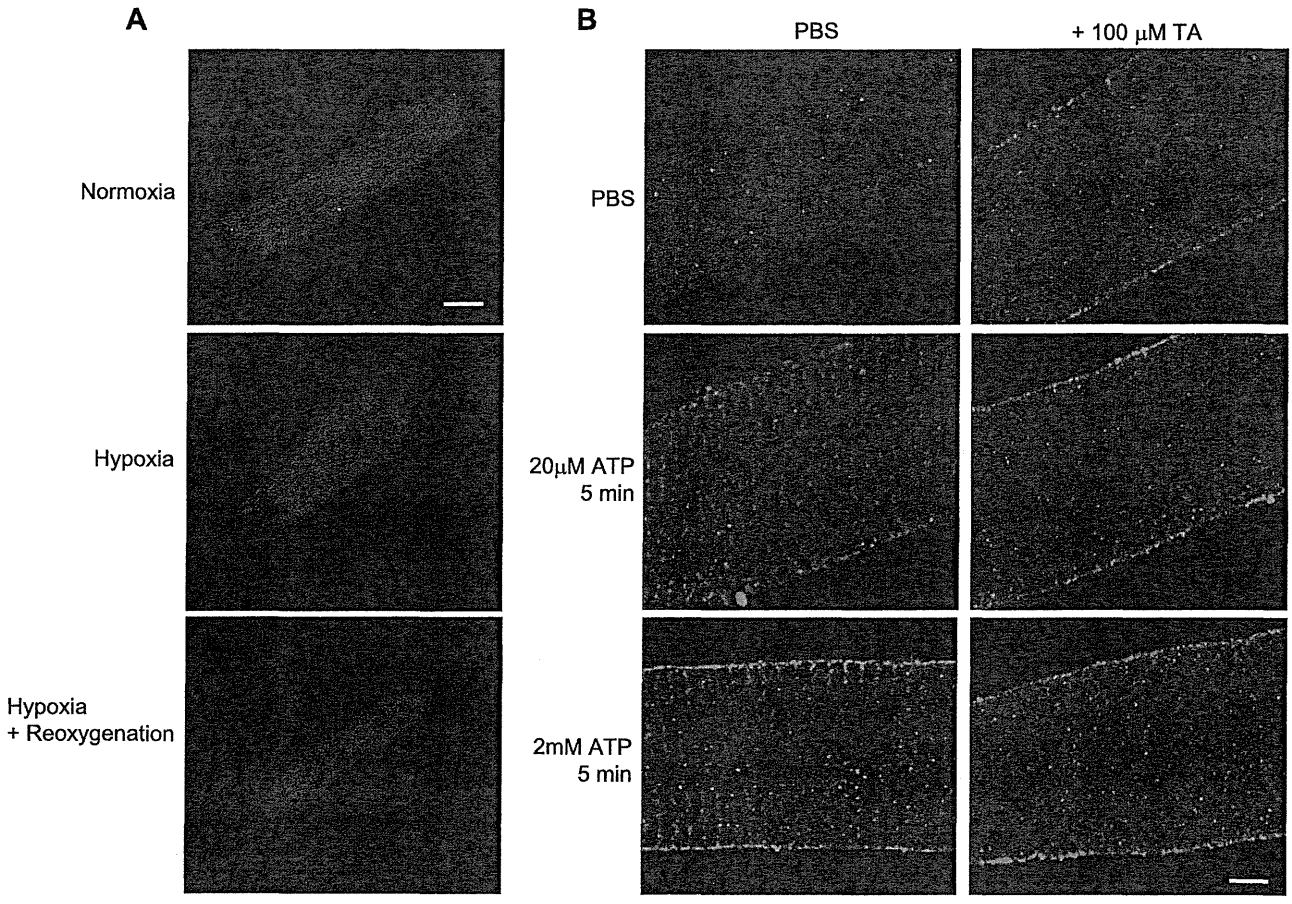

Fig. 4. Tec exhibits a striated localization pattern after adenine nucleotide stimulation. Adult mouse myocytes were isolated and cultured for 24 h, after which they were subjected to hypoxia alone (95% N_2-5% CO_2 for 1.5 h), hypoxia plus 1.5 h of reoxygenation, or ATP/adenosine stimulation. Tec localization was then evaluated by immunolabeling and confocal microscopy. *A*: hypoxia alone or with reoxygenation produced no discernable alterations in Tec localization. *B*: ATP stimulation induced Tec translocation to structures resembling T-tubular striation (*left*; adenosine treatment produced similar effects, not shown). PBS vehicle was used as a control. Inhibition of Tec with terreic acid (TA) blocked this translocation (*right* panels). Bar = 5 μm. Please see Supplemental Fig. 5 for lower-magnification images.

Supplemental Fig. 1).[1] To further test this possibility, we examined Tec expression in a model of ischemia-reperfusion injury in the mouse as well as in isolated myocytes after culture.

Ischemic injury, but not the cardiac protective agent DETA/NO, induces the translocation of Tec. To explore the role of Tec in normal and diseased hearts, we used an established model of regional myocardial ischemia and pharmacological cardiac protection. Thirty-minute ligation of the LAD followed by 24-h reperfusion produced myocardial infarction in Balb/c mice (31.68 ± 6.2% region at risk; Fig. 2*B*). Pretreatment with four intravenous boluses of DETA/NO (Fig. 2*A*) recapitulated the well-documented cardiac protective effect of this NO donor (infarct size was 15.1 ± 2.9% region at risk; Fig. 2*B*), as previously demonstrated with other mouse strains (28) and originally described in rabbits (23). Region at risk measurements were not significantly different between the two groups (data not shown).

To evaluate Tec abundance, we repeated the ischemic injury experiments in another cohort of mice and divided the hearts postmortem into nonischemic and ischemic regions based on the location of the LAD ligature. As such, the apex region was considered ischemic and the base nonischemic. After 30 min of ischemia and 24 h of reperfusion (the time of infarct size analysis), there was a modest (19.2%) but significant decrease in Tec abundance (blots in Fig. 3*A* and quantification in Fig. 3*B*). However, we observed a much greater decrease (43.9%) in Tec abundance after only 30 min of reperfusion, whereas there was no difference from control after 4 h of reperfusion or after treatment with DETA/NO. Strikingly, these changes took place only in the ischemic region (open bars) and not in the nonischemic region (solid bars) of the heart (Fig. 3*B*).

To our knowledge, there is no evidence of a tyrosine kinase undergoing such rapid degradation, and, in support of this, cardiac injury did not produce any lower-molecular-weight species of Tec protein as detected by Western blot analyis. Our initial experiments (Fig. 3, *A* and *B*) were performed in Triton X-100, in which lipid rafts are insoluble. To test whether Tec may be localizing to these rafts, which have been shown to be important compartments for cardiovascular signaling (17), hearts were homogenized in Triton X-100 lysis buffer with or without the addition of 0.6% CHAPS and 0.1% deoxycholate. Lysates were mixed with 80% sucrose, on top of which equal volumes of 35% and 5% sucrose were successively layered. After ultracentrifugation (18 h at 240,000 *g*), each tube was divided into eight fractions, where the first fraction was the lowest density and the eighth fraction was the highest density. Immunoblot analysis with anti-Tec demonstrated two populations of Tec: one associated with lighter membrane-enriched fractions and the other associated with denser protein-rich fractions (Fig. 3*C*, *top*). The addition of CHAPS and deoxycholate, detergents known to solubilize membrane proteins, resulted in the loss of the membrane-associated Tec population (Fig. 3*C*, *bottom*).

Purinergic stimulation, but not hypoxia, induces translocation of Tec in cardiac cells. Having established the activation of Tec in the ischemic myocardium, we sought to further explore the triggers for its translocation at the cellular level. Because a major injurious component of ischemia is hypoxia, we first examined the effect of this stress on Tec localization. Myocytes were isolated as described above, cultured for 24 h,

[1] Supplemental Material for this article is available online at the *American Journal of Physiology-Heart and Circulatory Physiology* website.

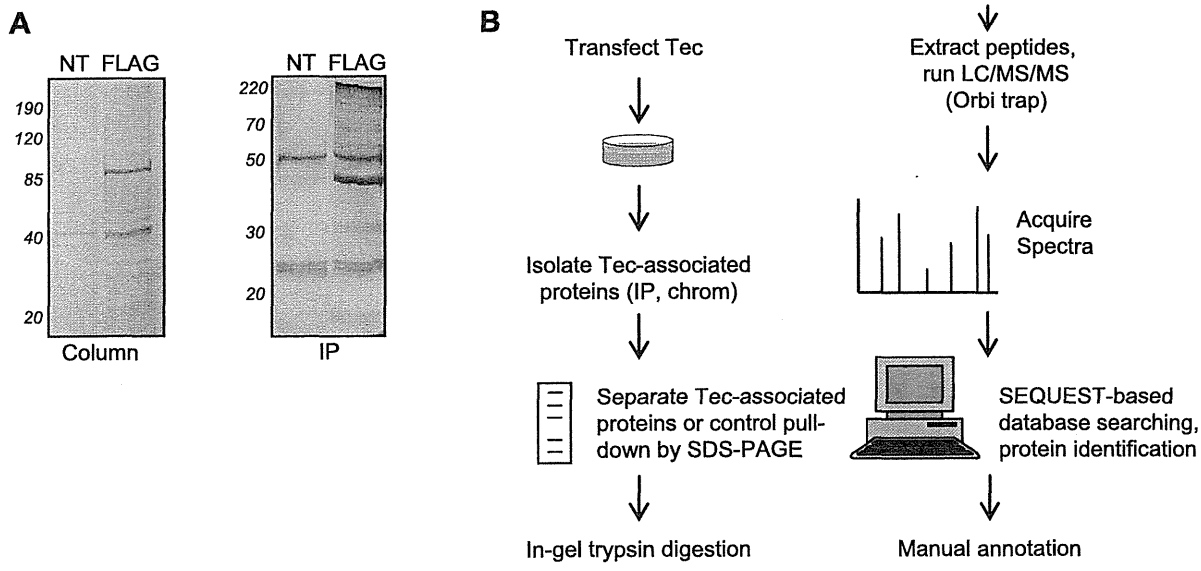

Fig. 5. Proteomic dissection of Tec tyrosine kinase signaling. *A*: Tec-associated proteins were purified by FLAG tag-based chromatography (*left*) or immunoprecipitation (IP; *right*). Cells transfected with nontagged Tec (NT) were used as a negative control. Proteins were separated by SDS-PAGE, and gels were stained with SYPRO. *B*: workflow for proteomic analyses. Human embryonic kidney-293 cells were transfected with pcDNA3 containing the Tec-COOH-FLAG insert (or pcDNA3 with untagged Tec as a control). Forty-eight hours later, cells were lysed and subjected to either FLAG IP using anti-FLAG-M2 antibody or column purification with FLAG affinity beads. Tec-associated proteins were separated by SDS-PAGE and stained with Coomassie blue. Protein bands were excised, digested with trypsin, and analyzed with liquid chromotography (LC)/mass spectrometry (MS)/MS on an Orbi-trap. Protein identification was carried out by database searching using the Sequest algorithm. Results from both purification processes were merged and then filtered.

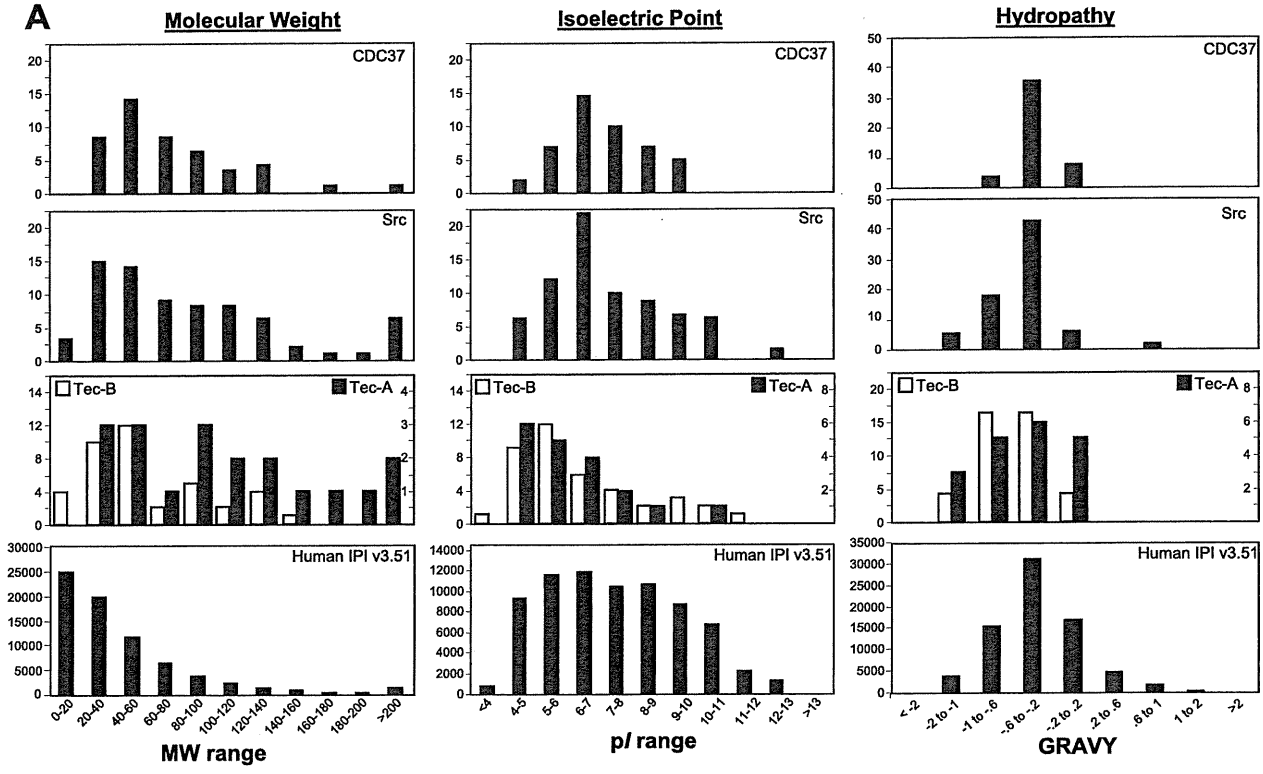

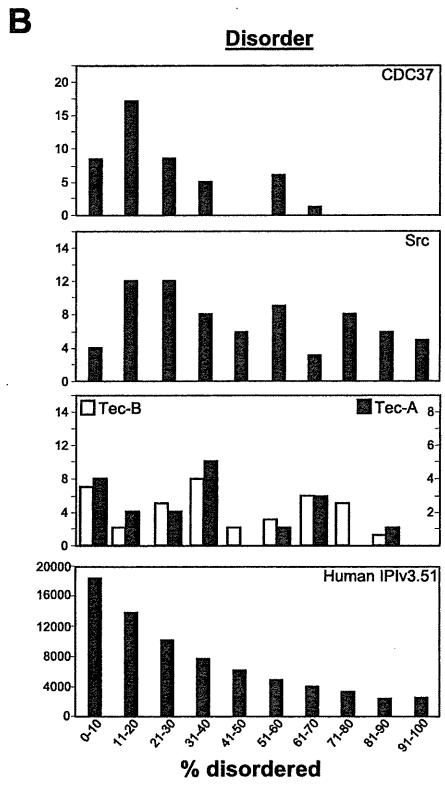

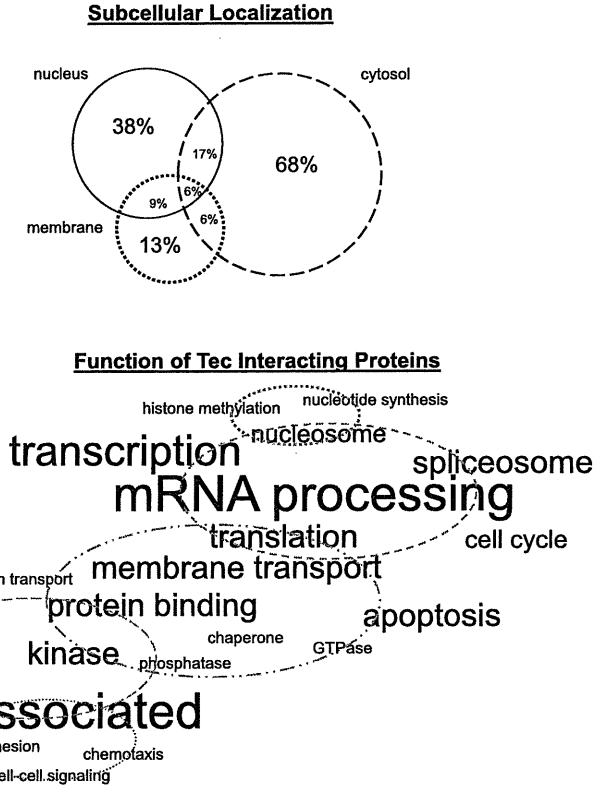

and placed in a hypoxic chamber flushed with 95% N_2-5% CO_2 for 1.5 h with or without 1.5 h of reoxygenation (room air). Hypoxia alone or with reoxygenation had no effect on Tec localization (Fig. 4*A*), although this same stimulus induced the nuclear localization of hypoxia-inducible factor (HIF)-1α in neonatal rat ventricular myocytes (Supplemental Fig. 2) and cell death, demonstrating that the hypoxic stimulus was sufficient to cause injury. Treatment with H_2O_2, to reproduce the ROS present during ischemia, also had no effect on Tec localization in the time courses we examined (Supplemental Fig. 3). However, purinergic stimulation by ATP (Fig. 4*B*) or adenosine (Supplemental Fig. 3) induced Tec translocation to striated structures resembling T-tubules. This translocation was inhibited by terreic acid, a Tec family PH domain inhibitor, implicating this domain of Tec in the interaction and supporting the role of lipid membranes in the altered association.

Unbiased mapping of Tec-interacting proteins by affinity isolation and LC/MS/MS. To better understand the in vivo signaling roles of the Tec family of tyrosine kinases, we used proteomic MS to examine proteins associated with the Tec isoform. Because it is abundantly expressed in the heart, we first sought to capture endogenous Tec interactors via immunoprecipitation from mouse hearts using an anti-Tec antibody. After MS analyses, this approach revealed many proteins specific to the Tec pulldown compared with the IgG control; however, the target itself (Tec) was not recovered at levels detectable by MS. We obtained similar results after immunoprecipitations for endogenous Tec from isolated mouse cardiac myocytes and fibroblasts. From a standpoint of protein interaction stoichiometry, we reasoned that while some of these interactors may be real, the isolation-detection approach was inappropriately selecting for abundant proteins. To overcome this limitation, we shifted our analyses to a HEK-293 cell-based system using a pcDNA3 vector containing Tec with and without a COOH-terminal FLAG tag. This approach afforded two methods of purification (Fig. 5): *1*) immunoprecipitation with anti-FLAG-M2-bound protein A/G beads and elution by boiling and *2*) column purification with FLAG affinity beads and competitive elution by 3× FLAG peptide. As a negative control, both types of FLAG purification were carried out on cells transfected with untagged Tec. Both methods of FLAG purification were performed in triplicate, and protein bands were examined along the continuum of the gel from experimental and control lanes. Importantly, this method allowed for MS identification of the target protein (Tec) at stoichiometric levels similar to the novel interactors we report below. Thus, while this method for protein identification was quite stringent and may have missed transient interactions, we feel that the rigor of this approach enhanced the validity of the results.

Tec interactors were filtered based on peptide count and analyzed with bioinformatics. Protein bands from Tec isolations (or untagged controls) were digested with trypsin and peptides analyzed by LC/MS/MS. Peptide spectra were searched against the human IPI database using the SEQUEST algorithm. To decipher distinct tiers of proteins interacting with Tec, we examined those detected with greater than or equal to five peptides or with greater than or equal to two peptides as indicators of the relative abundance of the protein in the Tec complexes (see the Supplemental Table for extensive experimental parameters on Tec-interacting proteins, including domain and functional annotation). In each case, we required that the protein was identified with the given number of peptides in more than one biological replicate (all identifications come from at least 2 technical and 2 biological replicates) and that the protein was not detected in the parallel negative control run. These experiments are the first to examine the signaling network of a member of the Tec family of tyrosine kinase using a nonbiased proteomic approach and provide the foundation for further studies of newly identified members of this network.

DISCUSSION

Since its discovery more than a decade ago, Tec tyrosine kinase has been the focus of extensive investigations in the immune system. Tec participates in proliferative signaling and differentiation in lymphocytes, whereas other members of the Tec family have been attributed specific signaling tasks in intracellular processes as varied as calcium signaling and apoptosis (19). Outside of the lymphocyte, however, the actions of Tec are less clear.

Several lines of evidence have pointed to a conserved role of nonreceptor tyrosine kinase signaling in cardiac growth and protection. However, the actions of the Tec family, in particular, have remained unexplored. One key study (4) has shown that Tec is activated in rat neonatal cardiomyocytes, whereas Bmx has been shown to participate in NO-induced cardiac protection (32) and pressure-overload-induced cardiac hypertrophy (14). We therefore hypothesized that Tec may be a stress-activated tyrosine kinase in the heart and have conducted extensive characterization of this isoform in the heart and isolated myocytes.

Role of Tec in myocardial ischemia. Tec protein is abundantly expressed in both the mouse heart and myocytes, in contrast to other members of the family, such as Bmx. To investigate whether the Tec isoform is involved in cardiac stress in vivo, we examined Tec abundance after ischemia-reperfusion in the mouse. Again, in contrast with Bmx (32),

Fig. 6. Subsets of interactors within the Tec signaling network. MS data were acquired on proteins associating with Tec (Fig. 5) and, after an analysis with distinct protein identification criteria, revealed two subsets of Tec interactors. *Subset A* was defined as interactors with *1*) identification by ≥5 peptides in ≥2 purification runs and *2*) never being identified (with 5 peptides) in a control run. *Subset B* was defined as interactors with *1*) identification by ≥2 peptides in ≥2 purification runs and *2*) never being identified (with 2 peptides) in a control run. *A*: physicochemical analysis of each tier of Tec interactor compared with the entire tandem MS-detectable proteome (as calculated from human IPI database version 3.51). Two other published experimental subproteomes with relevance to Tec signaling, Src (2) and CDC37 (20), are shown for comparison. MW, molecular weight; p*I*, isoelectric point; GRAVY, grand average of hydropathy. *B*: percentages of disordered regions in individual proteins from the various proteomes in our study as predicted by the DISOPRED2 algorithm. *C*: based on the UniProt annotations of *subset A* and *B* proteins, subcellular localization and protein function were visually represented. In the Venn diagram, percentages correspond to the portion of interactors with annotated localization in the three cellular compartments enriched in this data set. In the word cloud, proteins are grouped with relevance to cellular processes, and the font size corresponds directly to the number of proteins with the given annotation.

Tec was unaltered by NO donors. However, ischemia induced a transient decrease in Tec abundance, and our data suggest that this results from an altered association of the protein with lipid membranes. Willey and others (30) have described a similar membrane translocation by Bmx in the pressure-overloaded feline myocardium. In support of this observation, confocal microscopy clearly revealed two distinct populations of Tec, in the myocyte—diffuse cytoplasmic and striated T-tubular—and showed that after the stress of myocyte isolation, Tec transiently relocates to the latter. It is interesting to speculate that this change at the cellular level recapitulates that changes in Tec abundance seen in the mouse heart, but additional studies with in vivo tracking of Tec over time will be necessary to test this hypothesis. Thus, Tec is clearly involved in the temporal response of the heart to ischemia-reperfusion. Because Tec is also expressed and active in inflammatory cells, an alternative explanation for the increase in Tec abundance that effectively returns the relative levels close to the uninjured baseline is an increased contribution of Tec protein to the myocardial lysate from inflammatory cells that have infiltrated the injured myocardium during reperfusion. Testing this interesting possibility will require future in vivo fate mapping studies that allow us to distinguish different cell types and to correlate Tec abundance in these cells.

Tec is not activated in myocytes stimulated by hypoxia or ROS. Having demonstrated the involvement of Tec in ischemia-reperfusion injury to the heart, we next sought to further explore the activation at the cellular level. Hypoxia and ROS are two injurious components of ischemic stress commonly used in isolated cells to simulate ischemia. To our surprise, neither hypoxia nor H_2O_2 in any of the treatment combinations we administered were sufficient to induce alterations in Tec intracellular localization detectable by microscopy. It remains an open question, however, as to how these stresses alter Tec enzymatic activity and association with intracellular signaling partners. It is interesting to note one Tec interactor we discovered is HIF-1α, a critical participant in hypoxic stress. While there have been no previous reports of this interaction, phosphatidylinositol 3-kinase has been shown to independently signal to Tec and lead to HIF-1α protein accumulation (15).

Tec is involved in purinergic stimulation. Adenosine and other purine nucleotides are released during ischemia-reperfusion (6). Bony et al. (4) made the observation that transfected Tec-green fluorescent protein displayed T-tubule localization in ATP-treated neonatal rat ventricular myocytes. The actions of endogenous Tec in the setting of adult cardiac myocytes, however, remains unknown. We observe T-tubular localization of endogenous Tec after ATP, similar to the observations of Bony et al., and documented, for the first time, the translocation of endogenous Tec in adult cardiac cells.

Tec is inhibited by terreic acid. Terreic acid was originally characterized as a direct Btk PH domain inhibitor (12). Although Itk inhibition has been concurrently reported at a higher inhibitor concentration, to our knowledge, the present study is the first to demonstrate that terreic acid inhibits Tec membrane translocation in isolated cells. Because the Tec and Btk PH domains are nearly identical, it is likely that this domain is necessary for Tec membrane localization. However, protein structure data on the Tec family remain sparse, and further research in this area is required to fully understand the mechanism of terreic acid inhibition of the Tec family kinase PH domain.

Defining the intracellular signaling actions of Tec. The FLAG-based affinity isolation approach presented here is reproducible, specific, and does not disrupt interactors that may be affected by antibody binding, as in the case with immunoprecipitation. The drawbacks of this approach include the use of a heterologous system, and so the observations we made in the present study for Tec interactors must be confirmed in distinct cell types of interest in the future. Another concern is that some interactors may have escaped our rigorous identification criteria either because they are present at substoichiometric levels (such as the known interactor Src, which was only identified with lower threshold search criteria) and/or have a transient association with Tec. The higher threshold list reported in the present study was arrived at by an unbiased analysis of the data from multiple independent biological and technical replicates, decreasing the likelihood of false positive identifications (see the Supplemental Table for detailed domain and functional annotation of Tec interactors). Additionally, while several of the Tec-interacting proteins in *subsets A* and *B* are shared, such as ArfGAP with coiled-coil, ankyrin repeat and PH domains (ACAP)-2 (a PH domain containing GTPase) and tropomodulin (an actin regulatory protein), most of these proteins are distinct between the two subsets. We interpret this observation as a result of the distinct identification criteria selecting for proteins with different types of association with Tec. *Subset A* is more stringent from the standpoint of requiring a greater level of total peptides to be included for positive identification (higher inclusion threshold) and thus would select based on the total abundance of the protein. In contrast, *subset B* is more stringent from the standpoint of requiring fewer peptides in a control run to eliminate the protein (lower exclusion threshold in negative controls) and thus would be expected to select for proteins with a greater specificity in their interaction with Tec (although perhaps with lower abundance). Future in vitro protein interactions studies will be required to test this conjecture, but these distinct levels of interactions are

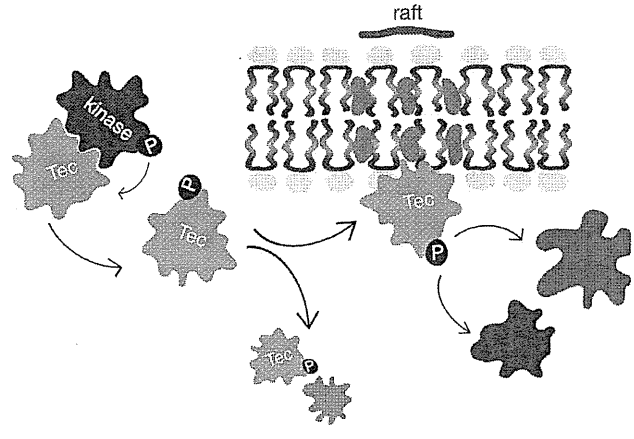

Fig. 7. Proposed mechanism of Tec signaling in the myocardium. A previous study (1) and our data suggest that stress-induced Tec activation is concomitant with a loss of regulation by phosphatases, followed by membrane localization. We propose that this translocation brings Tec into apposition with signaling partners, some of which have been identified in the present study.

presented here to give the most information about Tec interactors along with the appropriate level of experimental confidence.

HIF-1α, identified as a Tec interactor in this study, is an important mediator of adenosine nucleoside-induced neuroprotection in hypoxia-stimulated PC12 cells (34). Since Tec is activated by adenosine nucleotide stimulation in cardiomyocytes, it may participate in HIF-1α signaling during cardiac protection. Another interactor, CDC37, is an emerging heat shock protein 90 cochaperone whose client proteins are predominantly kinases (20). Also among the interactors we found was Rho kinase 1 (ROCK1), an immediate downstream kinase effector of RhoA GTPase. A recent knockout study (33) has indicated a critical role for ROCK1 in reactive fibrosis during pressure-overload hypertrophy. The specifics of how Tec may contribute to this process are unclear, but this observation is consistent with Tec's proliferative role in cell signaling and its abundant expression in fibroblasts. Finally, we found many structural proteins, such as ankyrin, spectrin, and clathrin, and many muscle contraction-associated proteins.

To mine for bioinformatic insights into the Tec subproteome, we examined how the physical-chemical properties of Tec interactors compare with the entire tandem MS-detectable proteome (i.e., the IPI database). The distributions of Tec interactors were not dramatically different from the IPI database for the metrics of molecular weight, isoelectric focusing point, and hydropathy score; however, Tec interactors differed significantly from the IPI database proteome in the area of protein disorder (Fig. 6), in which the Tec subproteome was populated by a significant number of proteins with extensive regions of disorder. Some investigators (29) have postulated that protein disorder is correlated with multifunctionality for protein interaction surfaces–the exact type used in signal transduction. It is worthwhile to note that Src (a homologous tyrosine kinase from a different family) and CDC27 (a Tec interactor identified in this study) subproteomes also had similar bias toward disorder.

We recognize that some of the most interesting aspects of the subproteome of Tec-associated signaling proteins remain unknown, including how it changes with stimulation and subcellular location. Indeed, these end points are the focus of ongoing work. However, the present study presents the first nonbiased analysis of Tec interactors in any cell type and sets the groundwork for the future investigation of cell- and stimulus-specific changes. Furthermore, we presented a rigorous and detailed methodological description of how protein interactions were determined (and false positives ruled out), which will inform future investigations of Tec and other signaling proteins via proteomics.

Summary and outlook. This study demonstrates the activation of endogenous Tec tyrosine kinase in mouse cardiac cells, illustrating similarities and differences with other Tec family members (Bmx in particular) as well as other nonreceptor tyrosine kinases from other protein families in myocardial ischemia and protection. This investigation provides the first global map of Tec-interacting proteins in any cell type. A model that emerges from this and other work is one in which a negative regulatory process (such as a tyrosine phosphatase) physically interacts with Tec kinase in an autoregulatory mechanism (Fig. 7) (25). Release from this cycle by stress stimuli allows Tec to associate with lipid membranes and regulate target proteins. Future studies will be necessary to test this model in detail in cardiac myocytes as well as to reveal the nuances of how Tec signals to different in vivo cellular targets.

GRANTS

This study was supported by National Heart, Lung, and Blood Institute (NHLBI) Grants HL-087132 and HL-096041 (to T. M. Vondriska), HL-088640 (to E. Stefani), and HL-080111 (to P. Ping) and the Laubisch Endowment of the University of California-Los Angeles (to T. M. Vondriska). M. J. Zhang received a scholarship from the University of California-Los Angeles Undergraduate Research Center. S. Franklin is the recipient of NHLBI Ruth Kirschstein Postdoctoral Fellowship F32-HL-091673.

DISCLOSURES

No conflicts of interest, financial or otherwise, are declared by the author(s).

REFERENCES

1. **Aoki N, Ueno S, Mano H, Yamasaki S, Shiota M, Miyazaki H, Yamaguchi-Aoki Y, Matsuda T, Ullrich A.** Mutual regulation of protein-tyrosine phosphatase 20 and protein-tyrosine kinase Tec activities by tyrosine phosphorylation and dephosphorylation. *J Biol Chem* 279: 10765–10775, 2004.
2. **Aranda B, Achuthan P, Alam-Faruque Y, Armean I, Bridge A, Derow C, Feuermann M, Ghanbarian AT, Kerrien S, Khadake J, Kerssemakers J, Leroy C, Menden M, Michaut M, Montecchi-Palazzi L, Neuhauser SN, Orchard S, Perreau V, Roechert B, van Eijk K, Hermjakob H.** The IntAct molecular interaction database in 2010. *Nucleic Acids Res* 38: D525–D531, 2010.
3. **Berglund L, Bjorling E, Oksvold P, Fagerberg L, Asplund A, Szigyarto CA, Persson A, Ottosson J, Wernerus H, Nilsson P, Lundberg E, Sivertsson A, Navani S, Wester K, Kampf C, Hober S, Ponten F, Uhlen M.** A genecentric Human Protein Atlas for expression profiles based on antibodies. *Mol Cell Proteomics* 7: 2019–2027, 2008.
4. **Bony C, Roche S, Shuichi U, Sasaki T, Crackower MA, Penninger J, Mano H, Puceat M.** A specific role of phosphatidylinositol 3-kinase gamma. A regulation of autonomic Ca^{2+} oscillations in cardiac cells. *J Cell Biol* 152: 717–728, 2001.
5. **Eble DM, Strait JB, Govindarajan G, Lou J, Byron KL, Samarel AM.** Endothelin-induced cardiac myocyte hypertrophy: role for focal adhesion kinase. *Am J Physiol Heart Circ Physiol* 278: H1695–H1707, 2000.
6. **Fox AC, Reed GE, Glassman E, Kaltman AJ, Silk BB.** Release of adenosine from human hearts during angina induced by rapid atrial pacing. *J Clin Invest* 53: 1447–1457, 1974.
7. **Haendeler J, Berk BC.** Angiotensin II mediated signal transduction. Important role of tyrosine kinases. *Regul Pept* 95: 1–7, 2000.
8. **Hakim ZS, DiMichele LA, Rojas M, Meredith D, Mack CP, Taylor JM.** FAK regulates cardiomyocyte survival following ischemia/reperfusion. *J Mol Cell Cardiol* 46: 241–248, 2009.
9. **Hattori R, Otani H, Uchiyama T, Imamura H, Cui J, Maulik N, Cordis GA, Zhu L, Das DK.** Src tyrosine kinase is the trigger but not the mediator of ischemic preconditioning. *Am J Physiol Heart Circ Physiol* 281: H1066–H1074, 2001.
10. **He Y, Luo Y, Tang SB, Rajantie I, Salven P, Heil M, Zhang R, Luo DH, Li XH, Chi HB, Yu J, Carmeliet P, Schaper W, Sinusas AJ, Sessa WC, Alitalo K, Min W.** Critical function of Bmx/Etk in ischemia-mediated arteriogenesis and angiogenesis. *J Clin Invest* 116: 2344–2355, 2006.
11. **Hirotani S, Higuchi Y, Nishida K, Nakayama H, Yamaguchi O, Hikoso S, Takeda T, Kashiwase K, Watanabe T, Asahi M, Taniike M, Tsujimoto I, Matsumura Y, Sasaki T, Hori M, Otsu K.** Ca^{2+}-sensitive tyrosine kinase Pyk2/CAK beta-dependent signaling is essential for G-protein-coupled receptor agonist-induced hypertrophy. *J Mol Cell Cardiol* 36: 799–807, 2004.
12. **Kawakami Y, Hartman SE, Kinoshita E, Suzuki H, Kitaura J, Yao L, Inagaki N, Franco A, Hata D, Maeda-Yamamoto M, Fukamachi H, Nagai H, Kawakami T.** Terreic acid, a quinone epoxide inhibitor of Bruton's tyrosine kinase. *Proc Natl Acad Sci USA* 96: 2227–2232, 1999.
13. **Mano H, Yamashita Y, Miyazato A, Miura Y, Ozawa K.** Tec protein-tyrosine kinase is an effector molecule of Lyn protein-tyrosine kinase. *FASEB J* 10: 637–642, 1996.

14. **Mitchell-Jordan SA, Holopainen T, Ren S, Wang S, Warburton S, Zhang MJ, Alitalo K, Wang Y, Vondriska TM.** Loss of Bmx nonreceptor tyrosine kinase prevents pressure overload-induced cardiac hypertrophy. *Circ Res* 103: 1359–1362, 2008.
15. **Mottet D, Dumont V, Deccache Y, Demazy C, Ninane N, Raes M, Michiels C.** Regulation of hypoxia-inducible factor-1alpha protein level during hypoxic conditions by the phosphatidylinositol 3-kinase/Akt/glycogen synthase kinase 3beta pathway in HepG2 cells. *J Biol Chem* 278: 31277–31285, 2003.
16. **O'Connell TD, Rodrigo MC, Simpson PC.** Isolation and culture of adult mouse cardiac myocytes. *Methods Mol Biol* 357: 271–296, 2007.
17. **Patel HH, Insel PA.** Lipid rafts and caveolae and their role in compartmentation of redox signaling. *Antioxid Redox Signal* 11: 1357–1372, 2009.
18. **Rajantie I, Ekman N, Iljin K, Arighi E, Gunji Y, Kaukonen J, Palotie A, Dewerchin M, Carmeliet P, Alitalo K.** Bmx tyrosine kinase has a redundant function downstream of angiopoietin and vascular endothelial growth factor receptors in arterial endothelium. *Mol Cell Biol* 21: 4647–4655, 2001.
19. **Schwartzberg PL, Finkelstein LD, Readinger JA.** TEC-family kinases: regulators of T-helper-cell differentiation. *Nat Rev Immunol* 5: 284–295, 2005.
20. **Smith JR, Workman P.** Targeting CDC37: an alternative, kinase-directed strategy for disruption of oncogenic chaperoning. *Cell Cycle* 8: 362–372, 2009.
21. **Takahashi-Tezuka M, Hibi M, Fujitani Y, Fukada T, Yamaguchi T, Hirano T.** Tec tyrosine kinase links the cytokine receptors to PI-3 kinase probably through JAK. *Oncogene* 14: 2273–2282, 1997.
22. **Takahashi N, Seko Y, Noiri E, Tobe K, Kadowaki T, Sabe H, Yazaki Y.** Vascular endothelial growth factor induces activation and subcellular translocation of focal adhesion kinase (p125FAK) in cultured rat cardiac myocytes. *Circ Res* 84: 1194–1202, 1999.
23. **Takano H, Tang XL, Qiu Y, Guo Y, French BA, Bolli R.** Nitric oxide donors induce late preconditioning against myocardial stunning and infarction in conscious rabbits via an antioxidant-sensitive mechanism. *Circ Res* 83: 73–84, 1998.
24. **Tang B, Mano H, Yi T, Ihle JN.** Tec kinase associates with c-kit and is tyrosine phosphorylated and activated following stem cell factor binding. *Mol Cell Biol* 14: 8432–8437, 1994.
25. **Tomlinson MG, Heath VL, Turck CW, Watson SP, Weiss A.** SHIP family inositol phosphatases interact with and negatively regulate the Tec tyrosine kinase. *J Biol Chem* 279: 55089–55096, 2004.
26. **Tomlinson MG, Kane LP, Su J, Kadlecek TA, Mollenauer MN, Weiss A.** Expression and function of Tec, Itk, and Btk in lymphocytes: evidence for a unique role for Tec. *Mol Cell Biol* 24: 2455–2466, 2004.
27. **Vondriska TM, Zhang J, Song C, Tang XL, Cao X, Baines CP, Pass JM, Wang S, Bolli R, Ping P.** Protein kinase C epsilon-Src modules direct signal transduction in nitric oxide-induced cardioprotection: complex formation as a means for cardioprotective signaling. *Circ Res* 88: 1306–1313, 2001.
28. **Wang G, Liem DA, Vondriska TM, Honda HM, Korge P, Pantaleon DM, Qiao X, Wang Y, Weiss JN, Ping P.** Nitric oxide donors protect murine myocardium against infarction via modulation of mitochondrial permeability transition. *Am J Physiol Heart Circ Physiol* 288: H1290–H1295, 2005.
29. **Ward JJ, Sodhi JS, McGuffin LJ, Buxton BF, Jones DT.** Prediction and functional analysis of native disorder in proteins from the three kingdoms of life. *J Mol Biol* 337: 635–645, 2004.
30. **Willey CD, Palanisamy AP, Johnston RK, Mani SK, Shiraishi H, Tuxworth WJ, Zile MR, Balasubramanian S, Kuppuswamy D.** STAT3 activation in pressure-overloaded feline myocardium: role for integrins and the tyrosine kinase BMX. *Int J Biol Sci* 4: 184–199, 2008.
31. **Xuan YT, Guo Y, Han H, Zhu Y, Bolli R.** An essential role of the JAK-STAT pathway in ischemic preconditioning. *Proc Natl Acad Sci USA* 98: 9050–9055, 2001.
32. **Zhang J, Ping P, Wang GW, Lu M, Pantaleon D, Tang XL, Bolli R, Vondriska TM.** Bmx, a member of the Tec family of nonreceptor tyrosine kinases, is a novel participant in pharmacological cardioprotection. *Am J Physiol Heart Circ Physiol* 287: H2364–H2366, 2004.
33. **Zhang YM, Bo J, Taffet GE, Chang J, Shi J, Reddy AK, Michael LH, Schneider MD, Entman ML, Schwartz RJ, Wei L.** Targeted deletion of ROCK1 protects the heart against pressure overload by inhibiting reactive fibrosis. *FASEB J* 20: 916–925, 2006.
34. **zur Nedden S, Tomaselli B, Baier-Bitterlich G.** HIF-1 alpha is an essential effector for purine nucleoside-mediated neuroprotection against hypoxia in PC12 cells and primary cerebellar granule neurons. *J Neurochem* 105: 1901–1914, 2008.

Immunology Letters 127 (2010) 135–142

Contents lists available at ScienceDirect

Immunology Letters

journal homepage: www.elsevier.com/locate/

Tec protein tyrosine kinase inhibits CD25 expression in human T-lymphocyte

Kentaro Susaki[a], Akira Kitanaka[b], Hiroaki Dobashi[a,*], Yoshitsugu Kubota[c], Katsuharu Kittaka[a], Tomohiro Kameda[a], Genji Yamaoka[b], Hiroyuki Mano[d], Keichiro Mihara[e], Toshihiko Ishida[a]

[a] Division of Endocrinology and Metabolism, Hematology, Rheumatology, and Respiratory Medicine, Department of Internal Medicine, Faculty of Medicine, Kagawa University, 1750-1 Ikenobe, Miki-cho, Kita-gun, Kagawa 761-0793, Japan
[b] Department of Laboratory Medicine, Faculty of Medicine, Kagawa University, 1750-1 Ikenobe, Miki-cho, Kita-gun, Kagawa 761-0793, Japan
[c] Department of Transfusion Medicine, Faculty of Medicine, Kagawa University, 1750-1 Ikenobe, Miki-cho, Kita-gun, Kagawa 761-0793, Japan
[d] Division of Functional Genomics, Jichi Medical University, 3311-1 Yakushiji, Shimotsuke-shi, Tochigi 329-0498, Japan
[e] Department of Hematology and Oncology, Research Institute for Radiation Biology and Medicine, Hiroshima University, 1-2-3 Kasumi, Minami-ku, Hiroshima 734-8553, Japan

ARTICLE INFO

Article history:
Received 16 July 2009
Received in revised form 21 October 2009
Accepted 23 October 2009
Available online 31 October 2009

Keywords:
Tec
CD25
T-lymphocyte

ABSTRACT

The Tec protein tyrosine kinase (PTK) belongs to a group of structurally related nonreceptor PTKs that also includes Btk, Itk, Rlk, and Bmx. Previous studies have suggested that these kinases play important roles in hematopoiesis and in the lymphocyte signaling pathway. Despite evidence suggesting the involvement of Tec in the T-lymphocyte activation pathway via T-cell receptor (TCR) and CD28, Tec's role in T-lymphocytes remains unclear because of the lack of apparent defects in T-lymphocyte function in Tec-deficient mice. In this study, we investigated the role of Tec in human T-lymphocyte using the Jurkat T-lymphoid cell line stably transfected with a cDNA encoding Tec. We found that the expression of wild-type Tec inhibited the expression of CD25 induced by TCR cross-linking. Second, we observed that LFM-A13, a selective inhibitor of Tec family PTK, rescued the suppression of TCR-induced CD25 expression observed in wild-type Tec-expressing Jurkat cells. In addition, expression of kinase-deleted Tec did not alter the expression level of CD25 after TCR ligation. We conclude that Tec PTK mediates signals that negatively regulate CD25 expression induced by TCR cross-linking. This, in turn, implies that this PTK plays a role in the attenuation of IL-2 activity in human T-lymphocytes.

1. Introduction

The activation and development of lymphocytes are regulated by the engagement of cell surface immune cell antigen receptors. Following receptor engagement, these receptors transmit signals by the activation of cytoplasmic protein tyrosine kinases (PTKs), such as Src, Syk, and Tec families [1,2]. The Tec family PTKs are nonreceptor PTKs including Tec, Btk, Itk (Emt/Tsk), Rlk (Txk), and Bmx (Etk). They are typically characterized by a pleckstrin-homology domain, a Tec-homology domain, Src homology domains (SH2 and SH3), and a kinase domain [3,4]. The biological importance of the Tec PTK subfamily was first confirmed in B-lymphocytes by the finding that Btk is essential for B-cell development [5,6] and that mutations in Btk cause X-linked agammaglobulinemia (XLA) in humans and B-cell defects in *xid* mice [7–10]. For T-cells, mice lacking Itk exhibited decreased numbers of mature thymocytes and reduced proliferative responses to both allogeneic major histocompatibility complex stimulation and T-cell receptor (TCR) cross-linking [11]. In addition, TCR-induced phosphorylation and activation of PLC-γ are reduced in T-cells lacking Itk [12]. According to early observations, it has been speculated that the functions of Btk and Itk are essentially related to B- and T-lymphoid development and activation, respectively, while Tec participates mainly in signaling pathways regulating myeloid cell growth and differentiation.

In our previous studies, we revealed Tec's contribution to antigen receptor signaling in B-lymphoid cells. Ligation of the B-cell receptor (BCR), CD19, and CD38 caused tyrosine phosphorylation of Tec and increased Tec PTK activity [13]. Tec's important role in B-cells was further confirmed by the generation of Tec/Btk double-deficient mice exhibiting an early block in B-cell development and a severe reduction in peripheral B-cell numbers [14]. In T-cells, TCR stimulation induces the activation of Itk [15], Rlk [16], and Tec [17]. In addition, the ligation of T-cell costimulatory receptor CD28 also activates Itk [18] and Tec [17]. In primary splenocytes from 5C.C7 TCR-transgenic mice, depletion of Tec using an antisense oligonucleotide treatment reduces IL-2 production in response to TCR ligation [19]. Studies using the Tec-transfected Jurkat human T-lymphoid cell line proposed the unique roles of Tec in T-cell activation [17,20]. However, purified T-cells from Tec-deficient mice were reported to have no apparent defects in TCR or CD28 signaling [14]. Thus, it is still an open question whether or not Tec is essential in the signaling pathway of T-lymphoid cells.

* Corresponding author. Tel.: +81 87 891 2145; fax: +81 87 891 2147.
E-mail address: hdobashi@med.kagawa-u.ac.jp (H. Dobashi).

0165-2478/$ – see front matter © 2009 Elsevier B.V. All rights reserved.
doi:10.1016/j.imlet.2009.10.009

In the present study we investigated Tec's role in human T-lymphoid cells using a Jurkat cell line stably transfected with a cDNA encoding Tec. We found that the expression of wild-type Tec inhibited the expression of CD25 induced by TCR cross-linking. Second, we observed that LFM-A13, a selective inhibitor of Tec family PTK, rescued the suppression of TCR-induced CD25 expression observed in wild-type Tec-expressing Jurkat cells. In addition, expression of kinase-deleted Tec did not alter the CD25 expression level after TCR ligation. We conclude that Tec PTK activity mediates signals that negatively regulate CD25 expression induced by TCR cross-linking in human T-lymphocytes.

2. Materials and methods

2.1. Reagents and cells

The rabbit polyclonal anti-Tec antibodies were previously described [13]. A monoclonal antibody to phosphotyrosine (PY99) and goat antisera to Tec were purchased from Santa Cruz Biotechnology (Santa Cruz, CA). Monoclonal anti-CD3 antibody (OKT3) was obtained from Janssen Pharmaceutical (Tokyo, Japan). Monoclonal anti-CD28 antibody was from Immunotech (Marseille, France). PE-conjugated anti-CD25 antibody and FITC-conjugated anti-CD69 antibody were from Dako (Glostrup, Denmark). LFM-A13 (a-cyano-b-hydroxy-b-methyl-N-(2,5-dibromophenyl) propenamide) was from Calbiochem (San Diego, CA). LFM-A13 was dissolved in dimethyl sulfoxide (DMSO) and aliquots were stored at −30 °C. The final concentration of DMSO was less than 0.5% for all experiments. DMSO at this concentration had no discernible effect on cell growth or surface marker expression profiles, including CD3 and CD25 expression (data not shown). All other agents were purchased from commercial sources.

The Jurkat human T-lymphoid cell line was a generous gift from Dr. D. Campana (St. Jude Children's Research Hospital, Memphis, TN). Jurkat cells were maintained in RPMI-1640 (Sigma, St. Louis, MO) with 10% fetal calf serum, L-glutamine, and antibiotics.

2.2. Immunoprecipitation, electrophoresis, and Western blotting

The cells were lysed in lysis buffer (50 mM Tris–HCl [pH 7.5], 150 mM NaCl, 1% [v/v] Triton X-100, 1 mM Na_3VO_4, 1 mM phenylmethyl-sulfonyl fluoride, 5 μg/ml aprotinin, 1 mM EDTA–2Na). Immunoprecipitation and Western blotting analysis were performed as described previously [13]. The experiments were repeated independently at least three times.

2.3. DNA constructs and electroporation conditions

The construction of pSR expression vector containing cDNA of wild-type Tec (TecWT) and kinase-deleted Tec (TecKD) has been described elsewhere [21]. Jurkat cells (5×10^6/experiment) were subjected to electroporation with 30 μg of pSR or pSR containing TecWT or TecKD, as described previously [22]. Transfected cells were selected after 2 weeks' culture in the presence of 5 μg/ml of blasticidin S hydrochloride (Funakoshi, Tokyo, Japan). Blasticidin-resistant clones were expanded and screened for Tec expression by means of immunoprecipitation and Western blotting. Individual clones were cultured and were analyzed as a mixture of clones to avoid clonal variations.

2.4. Stimulation of T cells

Anti-CD3 antibody (2 μg/ml) was incubated in 24-well flat-bottom plates at 4 °C for 16 h for immobilization to the bottoms of the plates. The plates were washed twice to remove excess antibodies. Cells were incubated in each well of anti-CD3-coated plates at 37 °C in 5% CO_2 with 90% humidity for indicated periods. At the termination of the cultures, the cells were harvested, suspended in PBS, and subjected to further analysis. The experiments were repeated independently at least three times.

2.5. Flow cytometric analysis

The surface phenotypes of the cells were examined by flow cytometry as described previously [23]. Briefly, collected cells were incubated with a specific fluorescent-conjugated monoclonal antibody or control mouse IgG on ice for 30 min. After two washes with PBS, cells were analyzed with an EPICS XL flow cytometry system equipped with EXPO32 ADC software (Beckman Coulter, Miami, FL). The experiments were repeated independently three times.

2.6. Quantification of IL-2

To measure IL-2 production, Jurkat cells were cultured in 24-well plates at 1×10^6 cells/ml, 1 ml/well and stimulated with 2 μg/ml anti-CD3 plus 2 μg/ml anti-CD28 monoclonal antibodies, or 50 ng/ml PMA and 1 μM ionomycin for the positive control cultures. After 24 h culture, IL-2 secreted in the culture supernatant was measured using Quantiflow Human IL-2 Immunoassay kits (BioE, St. Paul, MN) according to the manufacturer's instructions. The experiments were repeated independently at least three times.

2.7. RT-PCR analysis

RT-PCR analysis was performed as described previously [24]. For amplification of the cDNA products, the following oligodeoxynucleotide primers were used: CD25 primers, 5′-GGGATACAGGGCTCTACACAG-3′ (sense) and 5′-ACCTGGAAACTGACTGGTCTC-3′ (antisense); β-actin primers, 5′-ATCATGTTTGAGACCTTCAA-3′ (sense) and 5′-GATGTCCACGTCACACTTCA-3′ (antisense). The PCR product was resolved by agarose gel electrophoresis and analyzed by means of densitometric analysis, and the fold increase in the CD25 cDNA level was normalized to the β-actin product. The experiments were repeated independently at least three times.

2.8. Statistical analysis

Data were analyzed by Student's *t*-test; $P < 0.05$ was considered to indicate a statistically significant difference.

3. Results

3.1. Ectopic expression and activation of Tec in Jurkat cells

As we reported previously, Jurkat cells lack endogenous Tec expression [13,25], making this cell line a useful model for studying the role of Tec in human T-cell biology. To investigate the role of Tec in human T-lymphoid cells, we introduced Tec cDNA to Jurkat cells. Clonal Jurkat cells expressing Tec protein (Jurkat-TecWT cells) were obtained after transfection and a subsequent series of limiting dilution procedures (Fig. 1a). In contrast, proteins in the anti-Tec immunoprecipitates from mock-transfected Jurkat cells (Jurkat-Mock cells) did not react with anti-Tec antibody (Fig. 1a). Ligation of TCR or CD28 is known to induce tyrosine phosphorylation of intracellular proteins in T-lymphoid cells, including Jurkat cell lines [1]. To determine whether or not the signaling pathways triggered by TCR or CD28 ligation were affected by the presence of Tec, intracellular protein tyrosine phosphorylation was analyzed by Western blotting using anti-phosphotyrosine antibody. As shown in Fig. 1b, in Jurkat-TecWT cells the ligation of CD3 or CD28 induced tyrosine phosphorylation with molecular weights and intensities

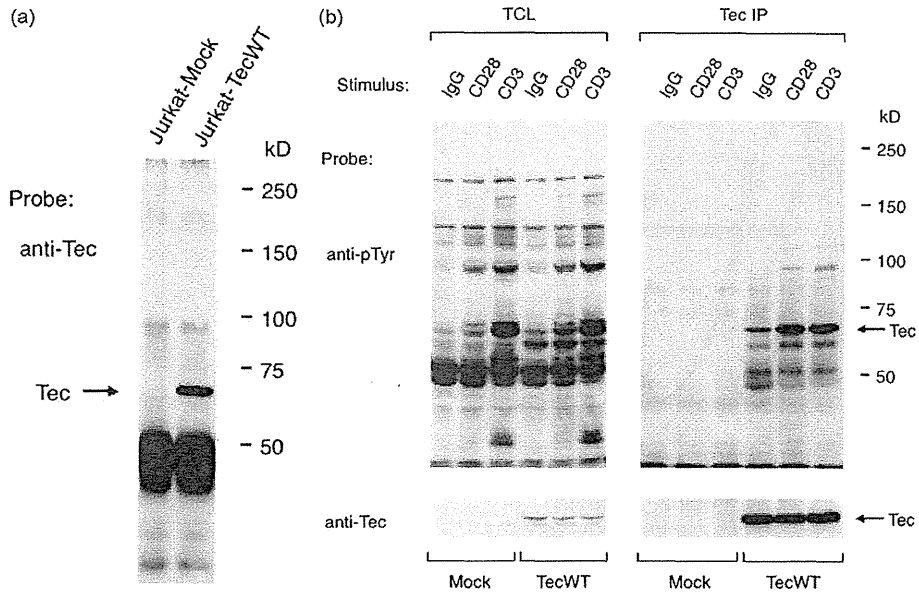

Fig. 1. Ectopically expressed Tec is activated following cell surface receptor cross-linking in Jurkat cells. (a) Cell lysates of Jurkat-Mock cells and Jurkat-TecWT cells were subjected to immunoprecipitation with anti-Tec antibody. Proteins were separated by SDS-PAGE and transferred to a PVDF membrane. The membrane was probed with anti-Tec polyclonal antibody. The positions of Tec and molecular mass markers (in kDa) are indicated. The intense band of approximately 50 kDa corresponds to the Ig heavy chain of the antibody used for immunoprecipitation. (b) Jurkat-Mock cells and Jurkat-TecWT cells were stimulated with control IgG, anti-CD28, or anti-CD3 for 5 min. Total cell lysates (TCLs) and proteins immunoprecipitated with anti-Tec (Tec IP) from these lysates were separated by SDS-PAGE and transferred to a PVDF membrane. The membrane was probed with anti-phosphotyrosine antibody (anti-pTyr; upper panel), then stripped and reprobed with anti-Tec polyclonal antibody (lower panel). The positions of Tec and molecular mass markers (in kDa) are indicated.

similar to those seen in Jurkat-Mock cells. Thus, the ectopic expression of Tec did not affect the overall profile and magnitude of the tyrosine-phosphorylated proteins, at least to an extent detectable by Western blotting. To determine whether or not TCR signaling activated transfected Tec in Jurkat cells, we examined Tec tyrosine phosphorylation after cross-linking the TCR with an anti-CD3 antibody. In contrast to the lack of a significant effect of Tec expression on the overall pattern of tyrosine phosphorylation, exposure to anti-CD3 antibody markedly increased tyrosine phosphorylation of Tec in Jurkat-TecWT cells (Fig. 1b). Stimulation of cells with anti-CD28 also triggered the tyrosine phosphorylation of Tec. Thus, activation of transfected Tec by ligation of T-cell-specific surface molecules was confirmed in Jurkat-TecWT cells. No tyrosine phosphorylation signal was detected in anti-Tec immunoprecipitates obtained from Jurkat-Mock cells (Fig. 1b).

We next examined the effect of Tec expression on Jurkat cell surface marker expression. The cell surface antigenic phenotype of Jurkat-TecWT cells was investigated by flow cytometry and compared with that of Jurkat-Mock cells. No apparent differences were observed in the expression of T-lymphoid cell markers and the activation markers examined, such as, CD1, CD2, CD3, CD4, CD8, CD25, CD28, and CD69, indicating that Tec expression had a minimal effect on the basal expression of representative T-cell surface proteins (data not shown).

3.2. Effect of Tec on IL-2 production

Because Tec overexpression in Jurkat cells has been reported to enhance IL-2 production and can induce TCR-mediated phospholipase Cγ (PLC-γ) phosphorylation and NFAT (nuclear factor of activated T-cells) activation [17,19,20,26,27], we attempted to replicate those findings with Jurkat cells stably transfected with Tec. Unexpectedly, exposure of Jurkat-TecWT cells to anti-CD3 plus anti-CD28 resulted in low levels of IL-2 production in both Jurkat-Mock cells and Jurkat-TecWT cells, without significant differences between the two cell types. In one experiment, after 24 h of incubation, 36 pg/ml IL-2 with anti-CD3 plus anti-CD28 stimulation versus 845 pg/ml IL-2 in control cultures with 50 ng/ml of PMA and 1 μM ionomycin were detected in the supernatant of the Jurkat-Mock cell culture, while 10 pg/ml IL-2 versus 850 pg/ml IL-2 was detected in the Jurkat-TecWT cell culture. Low IL-2 secretion in response to TCR stimulation was reproduced in both cell lines in repeated experiments. The addition of IL-2 at concentrations below 100 pg/ml had no influence on CD25 expression in either Jurkat-Mock cells or Jurkat-TecWT cells (data not shown).

3.3. Tec downregulates CD25 expression

CD25 is an essential component of high-affinity IL-2 receptors [28,29]. Although several investigators have proposed the possibility that Tec is involved in the IL-2-producing machinery [4,17,19,20,26,27,31,32,35], little is known about the relationship between Tec family PTK and CD25 expression, except the downregulation of CD25 observed in stimulated T-cells from Itk-deficient mice [12]. We evaluated the effect of Tec expression in Jurkat cells on CD25 expression. The membrane expression of CD25 increases after T-lymphocyte activation [28,29]. To examine whether or not Tec expression modifies TCR-mediated signaling, we examined changes in CD25 surface expression on Jurkat-derived clones activated for 24 h with TCR cross-linking using flow cytometry. As shown in Fig. 2a , enhanced CD25 expression was observed in Jurkat-Mock cells after the 24 h incubation with plate-bound anti-CD3. In contrast, the expression of CD25 after TCR cross-linking was markedly suppressed in Jurkat-TecWT cells (Fig. 2a). The percentage of CD25-expressing cells after TCR cross-linking was 39.5% in Jurkat-Mock cells and 9.9% in Jurkat-TecWT cells. These findings suggest that activation of Tec kinase results in the downregulation of CD25 expression induced by TCR cross-linking. CD69 (an activation-inducer molecule) is also known to be upregulated upon T-cell activation [1,12]. Next, we examined the effect

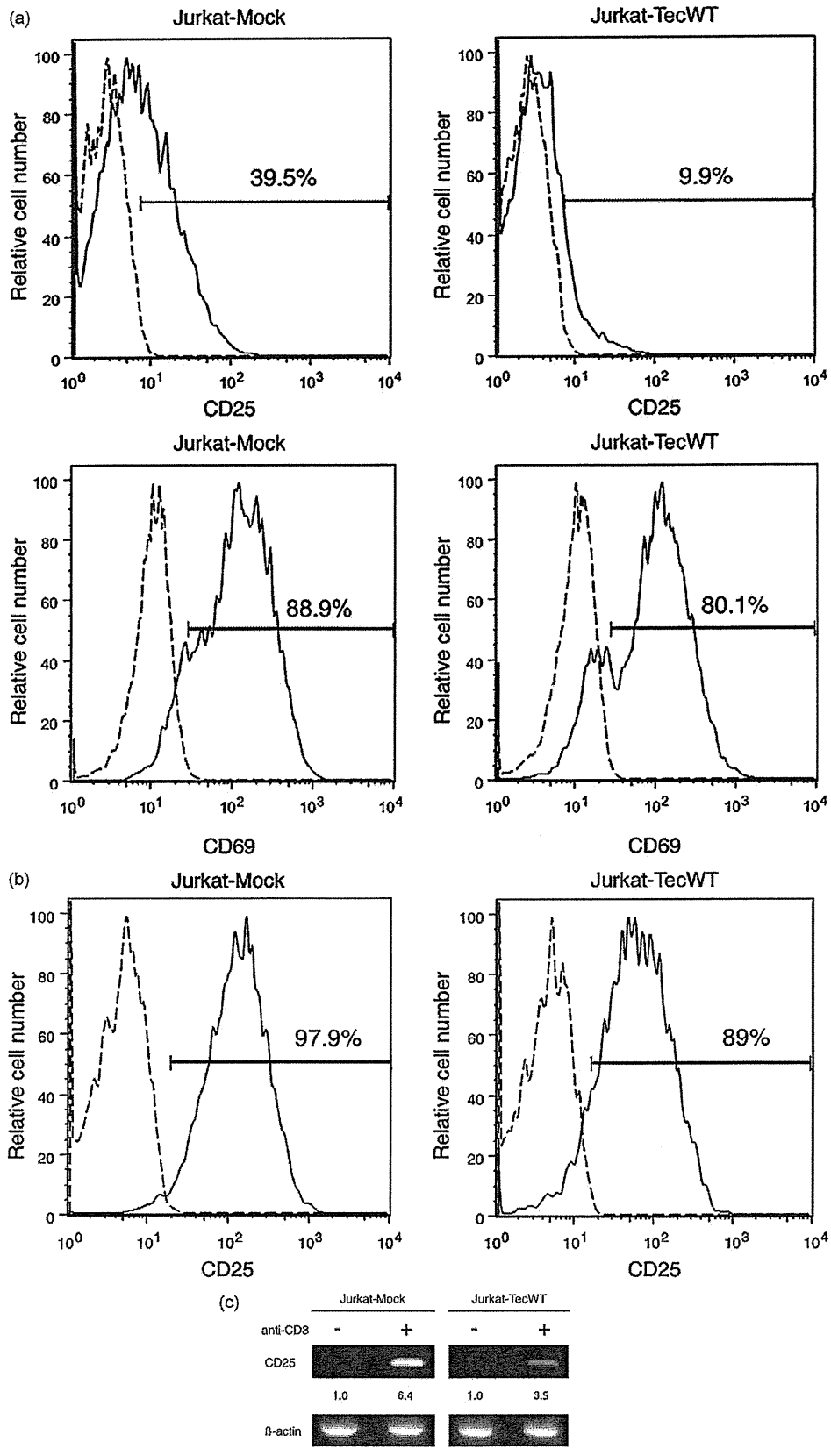

Fig. 2. Expression of Tec inhibits upregulation of CD25 but not that of CD69 induced by TCR cross-linking. (a) Jurkat-Mock cells and Jurkat-TecWT cells after TCR cross-linking were incubated with anti-CD25 (upper panels) and anti-CD69 (lower panels) antibodies. Flow cytometric histograms show the intensity of staining with the indicated antibody (solid line) compared with that of an isotype-matched nonreactive control antibody (broken line). (b) Jurkat-Mock cells and Jurkat-TecWT cells cultured

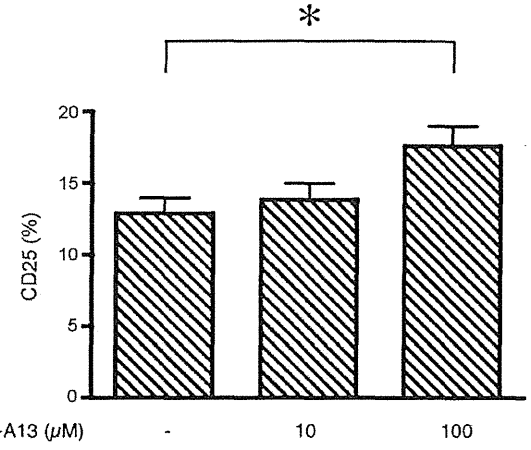

Fig. 3. Tec selective inhibitor LFM-A13 increases the CD25 expression on Jurkat-TecWT cells after TCR cross-linking. Jurkat-TecWT cells were treated with the indicated concentrations of LFM-A13 or DMSO (vehicle) for 1 h. The cells were then stimulated with TCR cross-linking for 24 h. CD25 expression was evaluated by means of flow cytometric analysis. Bars (mean ± SD of quadruplicate tests) represent the percentage of cells expressing CD25. *$P < 0.05$.

of Tec expression on the induction of CD69 caused by TCR cross-linking. Although CD25 expression was markedly suppressed after TCR stimulation in Jurkat-TecWT cells, no apparent difference was observed on the CD69 expression between Jurkat-Mock cells and Jurkat-TecWT cells (Fig. 2a). Thus, Tec expression inhibited CD25 expression after TCR cross-linking, without affecting CD69 induction. The defect in the signal seems to be adjacent to TCR, as Tec expression does not affect the CD25 expression level in Jurkat cells after PMA plus ionomycin activation, which bypasses the early stage signals induced by TCR cross-linking (Fig. 2b).

CD25 gene expression is tightly regulated at the transcriptional level [28,29]. Therefore, we next investigated the expression of CD25 mRNA in Jurkat-derived clones. Using RT-PCR, we examined the effect of TCR cross-linking on CD25 mRNA expression in Jurkat clones. As shown in Fig. 2c, CD25 mRNA expression in Jurkat-Mock cells was increased after 24 h stimulation with TCR cross-linking. In contrast, the increase in CD25 mRNA expression in Jurkat-TecWT cells after TCR cross-linking was markedly suppressed. The densitometric analysis of the relative intensities (means ± S.E.) of three independent experiments showed significant inhibition of the CD25 mRNA expression in Jurkat-TecWT cells after TCR cross-linking ($P < 0.05$) (data not shown). These results imply the importance of Tec PTK on the downregulation of CD25 expression after TCR cross-linking.

To further elucidate the contribution of Tec PTK activity on the results obtained by comparing Jurkat clones with or without Tec, we took advantage of LFM-A13, a compound that preferentially inhibits the enzymatic activity of Tec family PTKs both *in vitro* and *in vivo* [30] in order to investigate Tec's role in the regulation of CD25 expression. We examined LFM-A13's effect on CD25 surface expression in Jurkat-TecWT cells after TCR cross-linking. LFM-A13 dose-dependently increased CD25 expression in Jurkat-TecWT cells after TCR cross-linking (Fig. 3). After 24 h of culture, 17.6 ± 2.8% of cells incubated with 100 μM LFM-A13 expressed CD25, versus 12.9 ± 2.1% of cells in control cultures. CD3 surface expression was not altered when measured after 1 or 24 h incubation of Jurkat-TecWT cells with LFM-A13 (data not shown). Thus, LFM-A13's effect was not due to the modulation of cell-surface CD3 expression. In Jurkat-Mock cells, CD25 surface expression induced by TCR cross-linking was not affected by the presence of LFM-A13 (data not shown).

To corroborate the results obtained using LFM-A13, we established stable transfectants of Jurkat cells expressing a kinase domain-deleted Tec (Jurkat-TecKD) (Fig. 4a). Although rapid and transient tyrosine phosphorylation of Tec was observed after ligation of TCR in Jurkat-TecWT cells, no detectable tyrosine phosphorylation was observed in TecKD protein obtained from Jurkat-TecKD cells throughout the time course examined (Fig. 4b). In Jurkat-TecKD cells, CD25 expression after TCR cross-linking was comparable to that of Jurkat-Mock cells (Fig. 4c and d). These results indicate that Tec PTK activity contributes to the downregulation of CD25 observed in TCR-stimulated Jurkat-TecWT cells.

4. Discussion

Studies of Tec family PTKs have begun to reveal the crucial roles of these kinases in transducing stimuli triggered by immune cell antigen receptors, such as TCR and BCR, regulating lymphoid cell development and activation [31,32]. Targeted disruption of Tec family PTK genes has revealed the unique roles of individual PTKs in lymphocyte signal transduction. In T-cells, Itk and Rlk play important roles in the TCR-mediated signaling pathway, which leads to the phosphorylation and activation of PLC-γ, an essential step in lymphoid cell activation [4,33–35]. Despite evidence suggesting Tec's involvement in TCR and CD28 signaling, Tec's role in T-lymphocyte remains unclear because of the lack of an overt defect in T-lymphocyte function in Tec-deficient mice [14]. Recent findings indicating that Itk and Rlk have nonessential roles in pre-TCR signaling in the thymus [36] may suggest that Tec has a compensatory effect on the lack of these kinases in T-cell development. In the present study, we attempted to address Tec's role in human T-lymphocyte function using Jurkat cells stably transfected with Tec-based constructs. We have demonstrated that Tec PTK activation results in the suppression of TCR-induced CD25 expression, implying that this PTK transmits signals attenuating IL-2 activity in human T-lymphocytes.

IL-2 transmits its effects via a high-affinity IL-2 receptor, which is composed of three transmembrane proteins (α, β, γc subunits) [28,29]. The binding of CD25 (α subunit) to the low-affinity IL-2R (β, γc subunits) increases affinity to IL-2, enhancing the cellular responses to the low concentration of IL-2. A very small population of circulating mononuclear cells expresses CD25 in normal human peripheral blood. After antigen-induced activation, CD25 was strongly expressed in human T-lymphocytes [28,29]. CD25 expression is induced not only by antigen-induced activation, but also by various mitogenic stimulations including cytokines such as IL-1, IL-2, IL-7, IL-12, IL-15, IL-16, TNF-α, TGF-β, and IFN-α [28,29]. There have been extensive studies of how CD25 expression is regulated in response to these stimuli. CD25 expression is believed to be controlled mostly at the stage of transcription regulation. Therefore, the promoter lesions of CD25 have been analyzed in detail, and multiple molecules regulating its transcriptional level have been identified [28,29]. In contrast, relatively little effort has been made to identify the PTK that plays a key role in CD25 expression after T-cell activation. Although a higher degree of CD25 upreg-

with 50 ng/ml of PMA and 1 μM ionomycin were incubated with anti-CD25 antibody. Flow cytometric histograms show the intensity of staining with anti-CD25 antibody (solid line) compared with that of an isotype-matched nonreactive control antibody (broken line). (c) Total RNA was isolated from Jurkat-Mock cells and Jurkat-TecWT cells with or without TCR cross-linking using anti-CD3 antibody. The expression of CD25 mRNA in the cells was analyzed by means of RT-PCR using specific primers as described in Section 2. The expression of β-actin was used as a control. The intensity of the CD25 mRNA band was measured by scanning densitometry and normalized to β-actin. The fold change in CD25 mRNA after TCR cross-linking is shown in comparison with the level in the unstimulated cells as the average of three independent experiments.

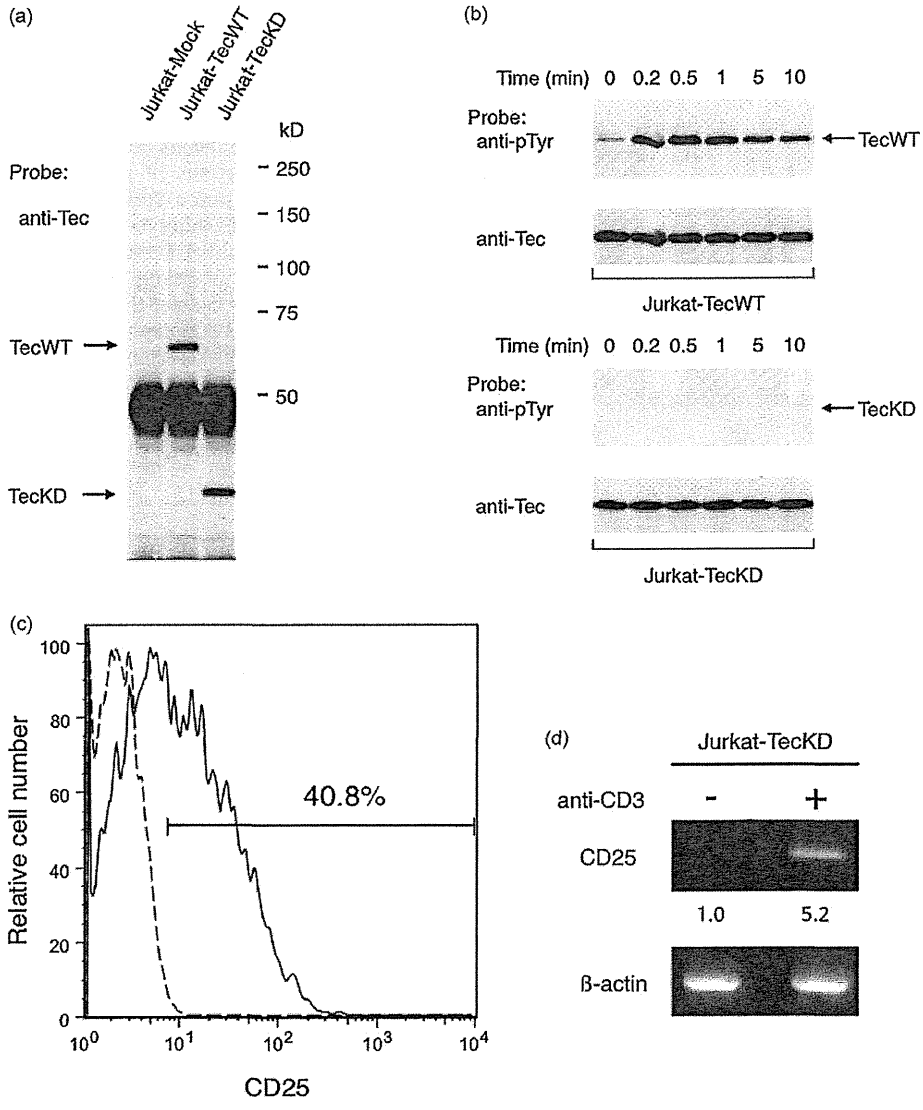

Fig. 4. Expression of Tec that lacks a kinase domain does not alter CD25 expression induced by TCR cross-linking. (a) Cell lysates of Jurkat-Mock cells, Jurkat-TecWT cells, and Jurkat-TecKD cells were subjected to immunoprecipitation with anti-Tec antibody and analyzed by Western blotting using anti-Tec antibody. The positions of TecWT and TecKD and molecular mass markers (in kDa) are indicated. The intense band of approximately 50 kDa corresponds to the Ig heavy chain of the antibody used for immunoprecipitation. (b) Jurkat-TecWT cells and Jurkat-TecKD cells were incubated with anti-CD3 antibody for the times indicated. Cell lysates were prepared and subjected to immunoprecipitation with anti-Tec antibody. The membrane was probed with anti-phosphotyrosine antibody (anti-pTyr; upper panel), then stripped and reprobed with anti-Tec polyclonal antibody (lower panel). The positions of TecWT and TecKD are indicated. (c) Jurkat-TecKD cells after TCR cross-linking were incubated with anti-CD25 antibody (solid line) or nonreactive control antibody (broken line), both conjugated to PE, and the fluorescence intensity was analyzed by flow cytometry. (d) Total RNA was isolated from Jurkat-TecKD cells with or without TCR cross-linking. The expression of CD25 mRNA in the cells was analyzed by means of RT-PCR using specific primers as described in Section 2. The expression of β-actin was used as a control. The intensity of the CD25 mRNA band was measured by scanning densitometry and normalized to β-actin. The fold change in CD25 mRNA after TCR cross-linking is shown in comparison with the level in the unstimulated cells as the average of three independent experiments.

ulation on wild-type T-cells compared with Itk-deficient T-cells was observed after TCR cross-linking, this difference is attributed to the IL-2-induced increase in CD25 expression, which is absent in Itk-deficient T-cells [12]. In our Jurkat system, the effect of Tec expression on IL-2 production was too small to alter CD25 expression level. The inefficient expression of CD25 in Jurkat-TecWT cells upon TCR stimulation seems to be dependent on the Tec PTK activity. Thus, the induction and activation of Tec in TCR-stimulated T-cells may impair the regulation of CD25 expression, resulting in the attenuation of IL-2-induced biological effects accomplished by autocrine and paracrine mechanisms. Prolonged upregulation of Tec relative to that of Itk in primary T-cells following anti-CD3 plus anti-CD28 stimulation [20] may imply that Tec has a negative regulatory role in the latter phase of the TCR-mediated signaling pathway. In human CD4+ T-cells, the Tec expression 24 h after TCR cross-linking was not altered (Susaki and Kitanaka, unpublished observation). Due to the difficulty of maintaining cell viability after sustained cell culture, we failed to examine the Tec expression level within the long time course in TCR-stimulated human CD4+ T-cells.

Previous studies using Jurkat cells have revealed that Tec overexpression enhances IL-2 promoter activity [17,19,26,27]. In our study, IL-2 production did not differ significantly between Jurkat-TecWT cells and Jurkat-Mock cells after anti-CD3 plus anti-CD28 stimulation. There is an apparent discrepancy between our find-